Transport scaling in incompletely chaotic Hamiltonian systems

Inaugural - Dissertation

zur

Erlangung des Doktorgrades der

Mathematisch-Naturwissenschaftlichen Fakultät

der Heinrich-Heine-Universität Düsseldorf

vorgelegt von

Dmitry Lesnik

aus Dnepropetrovsk

Düsseldorf

2002

Gedruckt mit der Genehmigung der Mathematisch-Naturwissenschaftlichen Fakultät der Heinrich-Heine-Universität Düsseldorf

Referent: Prof. Dr. K.-H. Spatschek

Koreferent: Prof. Dr. A. Pukhov

Tage der mündlichen Prüfungen: 16.05.02, 17.05.02, 22.05.02

Contents

1 Introduction

1.1 Motivation: The magnetic field in a fusion reactor

Since the discovery of the nuclear fusion, a very attractive idea of physics was to harness the energy released in the fusion reaction of two hydrogen atoms. It would be an almost inexhaustible energy source with less pollution and a smaller risk factor in comparison to other energy sources. Therefore, the realization of controlled fusion has become a challenge to science, since there are many physical and technical problems that have to be solved.

One of the most significant difficulties of the controlled fusion is the Coulomb repulsion: In order to fuse, two kernels need to overcome the electrostatic potential barrier between them. The probability for this process depends strongly on the system's conditions and it is possible to calculate a criterion under which the fusion reaction can take place. To be more specific, we look at the fusion of deuterium ${}^2_1D$ and tritium ${}^3_1T$. This process is usually considered as it has the largest cross-section and energy output. Any fusion process should run fast enough to compensate the energy escape. Thereto a sufficiently high density n is necessary to be kept for long enough time τ. For the $D-T$ reaction the Lawson-criterion [1] is

$$n \cdot \tau \cdot T \gtrsim 10^{20} \frac{s}{m^3} \cdot 3 \cdot 10^7 K \,,$$

and for a different process, the $D-D$ reaction, the Lawson number is even higher: $10^{22} s\, m^{-3} \cdot 10^8 K$.

There are two common ways to reach the threshold Lawson number:

- *inertial fusion*, which deals with strongly compressed deuterium-pellets and reaches the Lawson number due to high density n.
- *magnetic confinement*, which deals with low densities, but high temperatures and long confinement times. The main direction of this group belongs to *Tokamaks* as well as *Stellarators*.

The magnetic confinement seems to be more hopeful, since it would allow control of the reaction rate.

The matter in a tokamak (or stellarator), due to high temperature, is strongly ionized. In the strong magnetic field the charged particles are moving approximately along magnetic field lines, tracing out a helical path around it. All possible magnetic field configurations are limited by the Maxwell equation $\nabla \cdot \mathbf{B} = 0$. Apart from that the magnetic lines should not hit the walls of the plasma container to avoid energy loss. The simplest topological configuration, satisfying these conditions, is toroidal.

The difference between tokamak and stellarator is that the stellarator in contrast to the tokamak has no toroidal symmetry. A confinement in stellarator may thus be achieved in a stationary magnetic field, while in a tokamak an additional poloidal magnetic field is produced by a toroidal plasma current.

Although a single charged particle, to the lowest order, follows field lines and thus should never escape from the fusion device, the behavior of plasma particles is quite different. In real systems one observes a transport of particles and energy from the inside of the device to the exterior, which leads to loss of particles density and heat and reduces the Lawson number. There are two mechanisms of the radial transport: First, the collisional transport, caused by collisions between electrons and ions with each other. This transport is diffusive, i.e. proportional to the density gradient. The second one, the collective transport, arises from collective effects and is due to the long-scale Coulomb interaction. This transport may be of much higher order and is called *anomalous transport*.

To obtain confinement of the plasma, the magnetic field must possess magnetic surfaces, i.e. the field lines must trace out a nested set of toroidal surfaces. They could prevent the particles from radial transport, and allow pressure and temperature gradient. However, in practice, it appears that magnetic surfaces can be destroyed by motion of particles itself. Regions with "wild" (chaotic) character of motion appear in the structure of magnetic field. Such chaotic regions lead to

the anomalous transport of particles.

As an example, Fig. 1 illustrates the behavior of the magnetic field lines in different regions. It presents a portrait of the magnetic field structure in a Dynamical Ergodic Divertor, plotted in radius-poloidal angle coordinates. The picture is obtained from numerical simulations. In this numerical experiment the magnetic structure has been purposely destroyed in the vicinity of the wall. Undestroyed magnetic surfaces are recognizable in the plot as continuous lines (arising from successive intersections of a single magnetic line with the plotted plane). The area between undestroyed curves is filled with points (quasi-)randomly and corresponds to the chaotic region of the magnetic field structure.

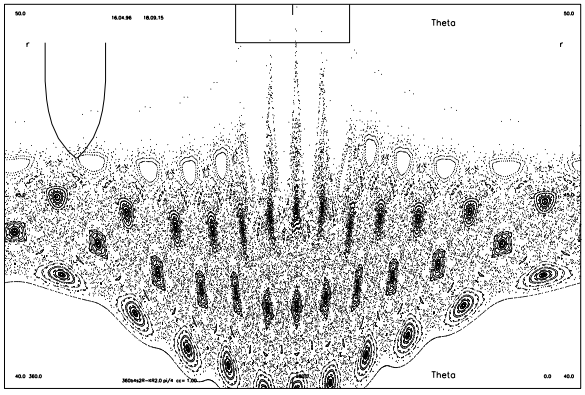

Figure 1: Cross section of the magnetic field structure in Dynamical Ergodic Divertor (DED).

The analytical description of a hot plasma embedded in a strong magnetic field is a difficult problem. But it is crucial for the design of any fusion reactor based on magnetic confinement. The aim of the present work is to contribute to its solution and to help to make the realization of controlled fusion possible.

1.2 Hamiltonian structure of a magnetic field

Because of its divergence-free property, the magnetic field flow can be formulated as a Hamiltonian system. Indeed, due to $\nabla \cdot \vec{B} = 0$, we can write $\vec{B} = \nabla \times \vec{A}$. Introducing the toroidal coordinates ρ, θ, ζ with $\vec{r}(\rho, \theta, \zeta)$, the vector potential may be written as:

$$\vec{A} = A_\rho \nabla\rho + A_\theta \nabla\theta + A_\zeta \nabla\zeta \,.$$

Then, we define $G(\rho, \theta, \zeta)$ so that $\partial G/\partial\rho = A_\rho$. Since $\nabla G = (\partial G/\partial\rho)\nabla\rho + (\partial G/\partial\theta)\nabla\theta + (\partial G/\partial\zeta)\nabla\zeta$, we can write

$$\vec{A} = \nabla G + \left(A_\theta - \frac{\partial G}{\partial\theta}\right)\nabla\theta + \left(A_\zeta - \frac{\partial G}{\partial\zeta}\right)\nabla\zeta \,,$$

or, introducing functions ψ and ψ_p,

$$\vec{A} = \nabla G + \psi\nabla\theta + \psi_p\nabla\zeta \,.$$

Thus, the magnetic field can be expressed in the form

$$\vec{B} = \nabla\psi \times \nabla\theta - \nabla\psi_p \times \nabla\zeta \,.$$

A magnetic field line is defined as a one parameter curve so that the magnetic field is everywhere tangent to it. Taking variables ψ, θ, ζ as new coordinates, we can choose ζ as a parameter on the curve $\{\psi(\zeta), \theta(\zeta)\}$. By definition of the tangent vector we have $\partial\psi/\partial\zeta = \vec{B}\cdot\nabla\psi/\vec{B}\cdot\nabla\zeta$, $\partial\theta/\partial\zeta = \vec{B}\cdot\nabla\theta/\vec{B}\cdot\nabla\zeta$. Substituting $\vec{B}$ from the last equation, we get

$$\frac{d\psi}{d\zeta} = -\frac{\nabla\psi\cdot(\nabla\psi_p\times\nabla\zeta)}{(\nabla\psi\times\nabla\theta)\cdot\nabla\zeta}\,, \qquad \frac{d\theta}{d\zeta} = -\frac{\nabla\theta\cdot(\nabla\psi_p\times\nabla\zeta)}{(\nabla\psi\times\nabla\theta)\cdot\nabla\zeta}$$

Writing the gradient of ψ_p as $\nabla\psi_p = (\partial\psi_p/\partial\psi)\nabla\psi + (\partial\psi_p/\partial\theta)\nabla\theta + (\partial\psi_p/\partial\zeta)\nabla\zeta$, we finally obtain:

$$\frac{d\psi}{d\zeta} = -\frac{\partial\psi_p}{\partial\theta}\,, \qquad \frac{d\theta}{d\zeta} = \frac{\partial\psi_p}{\partial\psi}\,.$$

These equations are of Hamiltonian form. A toroidal coordinate ζ plays then a role of time, and $\psi_p(\psi, \theta, \zeta)$ the Hamiltonian. A magnetic line corresponds to a

trajectory of the Hamiltonian system with appropriate initial conditions. Thus, the problem of *magnetic field lines transport* can be treated in the framework of the theory of Hamiltonian systems. The essential nonlinear nature of these equations makes the mathematical treatment of the problem extremely complicated [2, 3, 4]. A brief outline of the basic principles of Hamiltonian mechanics is given in App. A.1.

There are three basic concepts which are essential for understanding of the dynamical behavior of nonlinear conservative systems. The first is the concept of *global symmetries* which serve to constrain the dynamical flow of the system to a lower dimensional surface in the phase space. Some of these global symmetries are obvious and are related to the space-time symmetries of the system. Others are not obvious and have been called "hidden symmetries" by Moser in 1979. When there are as many global symmetries as degrees of freedom, the dynamical system is said to be integrable.

The second important concept is that of *nonlinear resonance*. Following a conjecture of Kolmogorov (1954), Arnol'd and Moser have in 1962 shown that, when a small symmetry-breaking term is added to the Hamiltonian, most of the phase space continues to behave as if the symmetries still exist. However, in regions where the symmetry-breaking term allows resonance to occur between otherwise uncoupled degrees of freedom, the dynamics begins to change its character. When resonances do occur, they generally occur on all scales in the phase space and give rise to an extremely complex structure.

The third important concept is that of *chaos* or *sensitive dependence* on initial conditions. For the class of systems in which symmetries can be broken by adding small symmetry-breaking terms, chaos first appears in the neighborhood of the nonlinear resonances. As the strength of the symmetry-breaking term increases and the size of the resonance regions increase ever larger regions of the phase space become chaotic.

The dynamical evolution of systems with broken symmetry cannot be deter-

mined using conventional perturbation theory, because of the existence of nonlinear resonances. Nonlinear resonances cause divergences in conventional perturbation expansions. This occurs because nonlinear resonances cause a topological change locally in the structure of the phase space and simple perturbation theory is not adequate to deal with such topological changes.

The problem of *anomalous transport* can be thought of as transport in a medium that is *strongly disordered*. The fine structure of phase space is the primary origin of anomalous transport in Hamiltonian systems. Long-range correlation effects occur from visits of orbits to boundary layers in the vicinity of islands (see below). The name "disordered" suggests that such systems are too complex for a detailed deterministic study: we have to resort to *statistical or probabilistic methods* for the study of such problems.

When the "degree of disorder" is very large, the system considered appears almost homogeneous on a macroscopic scale. This makes the statistical treatment very efficient. In an extremely disordered system, when a characteristic "stochasticity parameter" is very large, the transport processes behave almost classically, although the transport coefficients depend on the stochasticity parameter (hence on the degree of disorder), and the driving mechanism is not collisional. Such processes are called *diffusive, but anomalous*.

A fundamental difference between "ideally disordered" systems, like Sinai billiard, and more realistic systems, like the standard map, is the existence of islands, making phase space a complicated mixture of small nonchaotic domains and stochastic regions. The presence of the islands implies much stronger deviations in long time asymptotics than can be described by simply a change in the diffusion constant. This phenomenon was named *"strange diffusion processes"* [5]. It may result in transport that is slower than the expected diffusive one (*subdiffusive regime*), or faster than the diffusive one (*superdiffusive regime*).

Strange transport is a very important problem, since it has many practical applications. It is also extremely difficult to treat, because it occurs in systems

that are neither ideally ordered, nor ideally disordered. There are extremely few exact analytical results available. In the majority of cases one has to resort to numerical simulations, which may suggest approximate mathematical models, that can be treated analytically (or semianalytically).

1.3 Transition to discrete time systems

In principle, the study of the evolution of a material system should start from the equations of motion. It is, however, known that these are, generically, non-integrable. Therefore, they must be solved numerically. But even this is usually impossible, because a minimal degree of precision requires constraints that are not realizable even with the most powerful modern computers. A widely used method consists then of replacing the differential equations of motion by a *map*, i.e. of replacing the continuous time description by a discrete one (see App. A.2).

Maps, originating from the Hamiltonian systems, inherit most of their remarkable properties. The most important for us is that the Hamiltonian maps preserve area and do not support attractors.

The class of area preserving maps usually discussed in literature are the so-called *twist maps* (see App. A.2). Twist maps are a class of area preserving maps on the plane which provide clear visualization of the many important features of nonlinear conservative dynamical systems with two degrees of freedom. They may be thought of to be an analytic representation of a Poincaré surface section of a torus (see App. A.1). For instance, this is usual way, how the magnetic field system can be reduced to a discrete map. Area preserving maps also stand on their own as describing the dynamical evolution of systems with discrete time steps.

When an integrable twist map is rendered non-integrable by a small perturbation, resonance can occur. It leads to appearing of finite chains of alternating hyperbolic and elliptic fixed points surrounded by nonlinear resonance zones. As

the strength of the perturbation is increased, the resonance zones grow, can overlap and form a chaotic sea. We thus distinguish integrable from nonintegrable twist maps. Birkhoff's fixed point theorem (see App. A.2.) describes changes that occur in an integrable map when its integrability is destroyed by a perturbation. These changes and the new behavior that occurs in nonintegrable maps is a topic of intensive discussions.

Most of examples of twist maps, that are of practical interest, appear to be nonintegrable. It is however often possible to represent a given map as a sum of integrable part and a perturbation, which vanishes as a parameter, named *stochasticity* or *control* parameter goes to zero. Although the canonical perturbation theory in nonintegrable case breaks down, there still exist methods of approximate describing of the chaotic dynamics in the limit cases of small, as well as large stochasticity parameter.

It is well known that, if the map is nonintegrable, a variety of orbits is possible: *cycles* (conditionally periodic orbits), *island chains* (encircling the cycles), *KAM tori*, and *chaotic orbits*. For a sufficiently small stochasticity parameter resonance zones (both chaotic and regular) are separated from one another by KAM tori. Thus in area preserving maps the KAM tori serve to isolate one region of the phase space from another. These surfaces play crucial role in the transport process, since they prevent particles from reaching arbitrary values of "action" p. Thereby they are also often referred to as *transport barriers*. A KAM torus is destroyed suddenly, as the mapping parameter increases, allowing trajectories to diffuse more or less randomly in the chaotic sea.

One of the most frequently occurring models in many different applications is the *standard map*, first introduced by Chirikov [6]. It describes the local behavior of nonintegrable dynamical systems in the separatrix region of nonlinear resonances [7, 2, 3, 4]. A problem that reduces locally to the standard map is the

diffusion of magnetic lines in a tokamak or stellarator [8, 9]. Written in the form

$$p_{\nu+1} = p_\nu - \frac{K}{2\pi}\cos 2\pi\theta_\nu \,, \tag{1}$$

$$\theta_{\nu+1} = \theta_\nu + p_{\nu+1} \,, \tag{2}$$

it has become a paradigm for the study of properties of chaotic dynamics in Hamiltonian systems. In spite of its apparent simplicity, it exhibits much of the complexity and canonical behavior of more complicated models.

The real number $K \geq 0$ is the *stochasticity parameter*. Figure 2 shows a plot of some phase trajectories of the standard map for the value of stochasticity parameter $K = 0.7$.

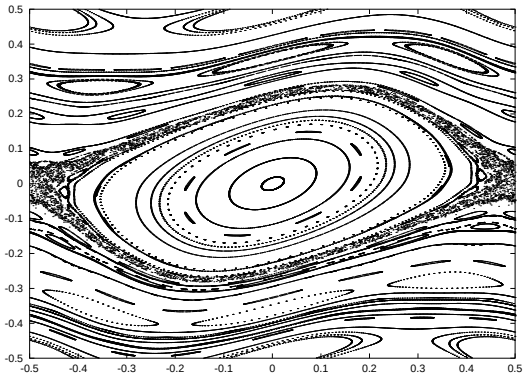

Figure 2: Standard map phase portrait for $K = 0.7$. The characteristic features, such as island chains, KAM surfaces, stochastic orbits may be clearly seen.

For small K, the chaotic component of the phase space is limited to finite regions, bounded by island chains and KAM barriers. As K gradually increases, the more subsequent KAM barriers are captured by chaotic component of phase space and thus destroyed. There exists a critical value, $K = K_c$, when the last ("golden") KAM barrier is destroyed, and the chaotic orbits can reach arbitrary values of p . The value of the critical K is $K_c = 0.971635....$ In the Fig. 3 we see phase portrait of the standard map for the value of stochasticity parameter above threshold, $K = 1.2$. Obviously, no primary KAM barriers are observed.

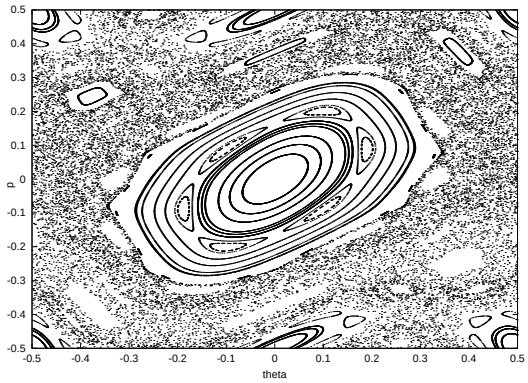

Figure 3: Standard map phase portrait for a $K = 1.2$. This is an above threshold regime, there are no more survived KAM tori present. A chaotic trajectory arising from the primary island separatrix may reach arbitrary values of p.

The method for obtaining the critical number of K was developed by Greene [10]. Each undestroyed orbit may be uniquely identified by its *winding number* w. At this correspondence every cycle M has a rational winding number, while KAM tori have irrational winding numbers. Since every irrational number can be approximated by a series of fractions, there is a way to approximate a torus by a sequence of cycles M_i. The method in question hinges on the fact that the existence of a KAM torus is related to the stability of the cycles which approximate it. It is assumed that if in the limit $i \to \infty$, the M_i-cycle has become unstable, the corresponding KAM torus itself has been destroyed. This behavior of the rational approximates provides a fairly precise method of determining numerically when a given KAM curve is destroyed. As the "most irrational" the golden mean number $[\gamma = (1 + \sqrt{5})/2]$ was supposed by Greene to be the winding number of the most stable KAM torus. Indeed, it has been numerically confirmed, that the golden mean, within numerical error, is the winding number associated with the last KAM curve to be destroyed in the standard mapping. Analyzing stability of the cycles, which approximate the "golden" KAM tori, the value K_c can be obtained.

We should note that in the area of stochastic magnetic field line transport, later some more sophisticated models than the standard map have been used [11, 12, 13, 14].

1.4 Anomalous transport

In the globally stochastic region of the phase space for a system with two degrees of freedom, in which KAM curves spanning the phase coordinate do not exist, a complete description of the motion is generally impractical. We can attempt to treat the motion in a statistical sense. That is, the evolution of certain average quantities can be determined, rather than the trajectory corresponding to a given set of initial conditions.

When a chaos sets in a twist map, large regions of the map can contain a "chaotic sea" of trajectories. There is no way to predict the future evolution of a trajectory in that region. However we can use the techniques of stochastic theory to determine the statistical behavior of trajectories. If the mapping parameter is large enough such that no stable islands or *cantori* exist, the diffusion process is very much alike to those found in simple Brownian motion. However, if stable islands and cantori exist, the diffusion process become much more complex.

Keeping in mind the application to the problem of magnetic field line diffusion in a tokamak, the interest usually lies in a reduced problem, namely the *"diffusion" in the radial direction*, which corresponds to the p direction in the standard map.

In numerous publications on transport in the standard map, the considerations concern only the transport in p direction. However, this map being asymmetric, it is of interest to consider both directions, p and θ, in transport computations [15]. In some physical applications, such as determining of heating rates and final energy distribution, one needs the angle evolution. Thus we distinguish between "action" and "angle" transport.

It is a well known fact that for a sufficiently large stochasticity parameter the standard map exhibits a diffusive behavior in the "action" direction. However, for some values of K, the system has a much more complicated dynamics. The presence of "survived" islands, surrounding stable periodical points, makes the phase space, in contrast to "pure stochastic" systems, a mixture of regular and chaotic components, causing a strong deviations from the diffusive law and appearing of anomalous transport. A reason for such deviations is the *stickiness property* of KAM surfaces: an orbit in a chaotic component, which comes close to a KAM surface bounding this component tends to spend longer time in its vicinity, and this time is typically longer the nearer the orbit comes.

A good (and usual) indicator of the dispersion is the *mean square displacement* (MSD): $\langle \Delta p^2(t) \rangle$ and $\langle (\Delta\theta)^2 \rangle$. (Here, $\langle \cdot \rangle$ means averaging over different initial conditions.) In its long time asymptotics $\nu \to \infty$, the stochastic system can be characterized by the transport exponents μ_p (for motion in p direction) and μ_θ (for motion in θ direction) that are defined through

$$\langle (\Delta p)^2 \rangle \sim \nu^{\mu_p} , \quad \langle (\Delta\theta)^2 \rangle \sim \nu^{\mu_\theta} , \tag{3}$$

respectively. Following the usual notation, the transport regime can be characterized as

$$\mu = 1, \text{ diffusive,}$$
$$\mu < 1, \text{ subdiffusive,}$$
$$\mu > 1, \text{ superdiffusive.}$$

It was shown that at some values of K the islands have strong effects on transport. For example, the two cases, K near the threshold $K_c \approx 0.972$ and K near $K_n = 2\pi n$, $n = 1, 2, \ldots$, respectively, were considered. In the latter case, relatively large accelerator mode islands lead to "peaks" of the transport exponent.

The complete description of the dispersion process would involve the determination of a "coarse-grained" *distribution function* $\psi(p, \theta; t)$. Its dynamics is

greatly simplified if an average over one of the variables can be employed. The applicability of this procedure has been explored by Lichtenberg and Lieberman [2] and is based on the random phase hypothesis.

In the section 2 our purpose will be to develop a semianalytical model for determination of the "action" distribution function $\psi(p;t) \equiv \langle \psi(p,\theta;t) \rangle_\theta$ in the subcritical regime $K < K_c$.

In the section 3 we use a Frobenius-Perron operator formalism to estimate the time evolution of the angular distribution $\psi(\theta;t) \equiv \langle \psi(p,\theta;t) \rangle_p$.

1.5 Transport in different regimes

1.5.1 $K < K_c$

It is clear *a priori* that the evolution process in the case $K < K_c$ *cannot be diffusive* in action space. Indeed, because of the presence of KAM barriers, the MSD will necessarily *saturate* asymptotically, as $t \to \infty$. The final value will be essentially the square of the width of the region occupied by the stochastic sea. This is in contrast with a diffusive process, in which the MSD exhibits an unbounded growth, proportional to time. The effective action diffusion coefficient (defined more precisely below) is thus necessarily zero:

$$D_p \sim \frac{d}{dt}\langle \Delta p^2(t) \rangle = 0. \tag{4}$$

We are thus in presence of a strongly *subdiffusive behavior*. Balescu and coworkers [11, 16] used a *continuous time random walk* model for subcritical values of the stochasticity parameter and have found a time asymptotic distribution in the thin stochastic layer of the separatrix region of the primary resonance island.

1.5.2 $K \sim K_c$

Maybe the most difficult region of the stochasticity parameter values for analytical treatment is that near the threshold $K_c \approx 0.972$. It has been intensively

investigated by White *et al.* [17]. An extremely complicated fine structure of the phase space has a strong influence on the trajectories behavior, making it essentially nondiffusive. Numerical simulations even show that an attempt to calculate a transport exponent is a nonconvergent process: there always present some irreducible uncertainty, depending on initial distribution, length of iterations, etc.

A starting point of the analysis of the transport in this case lies in the scaling behavior of "noble" tori. Kadanoff [18] and Shenker [19] were first who have shown that the cycles which approximate the KAM torus and the resonance zones associated with them exhibit scaling behavior and in some regions of the phase space form a self-similar structure. The scaling behavior of area preserving mappings has been extensively studied by many authors [20, 21, 22, 23].

MacKay [24] has developed a renormalization group theory for the noble KAM tori. On the basis of this approach many analytical predictions concerning transport rates in the vicinity of self-similar island chains can be done. A quantitative theory for the transport has been proposed using a fractional generalization of the diffusion (Fokker-Planck-Kolmogorov) equation [25]. The renormalization group has been used to obtain an explicit expression for the transport exponent.

In the centre of attention of many authors was a superdiffusive transport caused by accelerator islands [26, 27, 28] (see also [25, 29, 15]). It has been shown that the anomalous exponents are related to the characteristic temporal and spatial scaling parameters of the island chains. This phenomenon is observed only for certain values of K, when sufficiently large accelerator mode islands exist.

1.5.3 $K \to \infty$

In the limit of large stochasticity parameter K, the standard map exhibits a *diffusive behavior* in the action variable p, with a quasioscillating diffusion constant D_p as a function of K. The latter was first numerically discovered by Chirikov [6].

Rechester and White [30] and Rechester *et al.* [31] used a probabilistic method

for the solution of the Vlasov equation for the distribution function of the "kicked rotor" system. The latter may be thought as a continuous time complement of the standard map. Authors have studied a propagator G of the distribution function in a Fourier space and found dominant terms of its power expansion with a small parameter $1/\sqrt{K}$. It was shown that for large K in a first approximation, the "action" diffusion coefficient D_p can be estimated as

$$D_p \approx \frac{K^2}{4}[1 - 2J_2(K)] \; . \tag{5}$$

where J_2 is the Bessel function of the first kind (and second order).

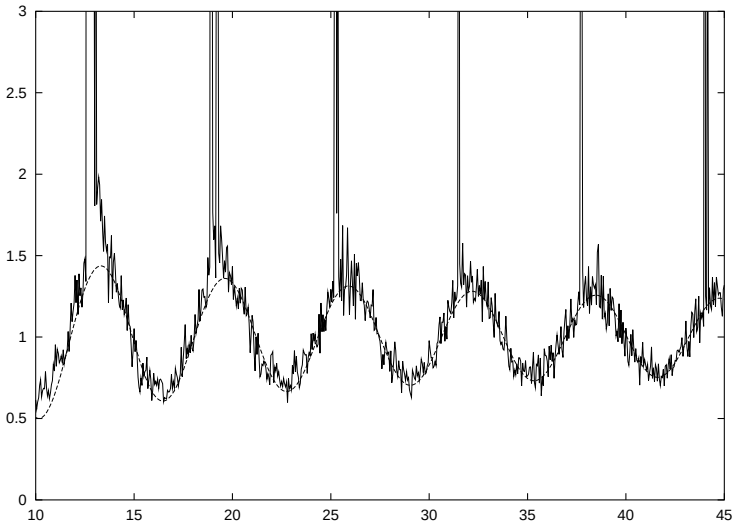

Figure 4: Diffusion coefficient D_p, normalized to the quasilinear result $D_{QL} = \frac{K^2}{4}$ vs the control parameter K. The smooth dotted curve shows an analytical first order estimate, obtained from a FP-operator expansion. Oscillations are due to correlations, which persist well above the chaotic threshold. Regular "peaks" are caused by trapping of orbits in the vicinity of accelerator mode islands.

Later, spectral properties of the discrete time evolution operator, named Frobenius-Perron (FP) operator, were rigorously studied. Many of its properties are known [32, 33, 34]. Hasegawa and Saphir [35, 34] have obtained a spectral

decomposition of the FP operator and shown, that the corresponding eigenvalues are related to the decay rates of correlation functions. These rates are the logarithms of the Ruelle resonances, which are defined as a poles of the resolvent of the FP operator.

Khodas and Fishman [36] and Khodas *et al.* [37] have found that the slow relaxation rates, in essence, correspond to diffusion modes in the momentum direction.

Bénisti and Escande [38] showed that the diffusion properties of the standard map are nonuniversal in the framework of the wave-particle interaction.

1.6 The subject of the present work

In the present work all the analyses was fulfilled on example of the standard map. The standard map may be written in action-angle variables p and θ,

$$p' = p - \frac{K}{2\pi}\sin 2\pi\theta\,, \tag{6}$$

$$\theta' = \theta + p'\,, \tag{7}$$

where K is the stochasticity (control) parameter. All values are then taken at discrete "times" ν, which correspond to values of the toroidal angle. The latter is assumed as nonperiodic while the poloidal angle is periodic, as denoted above [30, 31, 16].

The topology of the Poincaré plots for sets of numerically iterated trajectories depends on the stochasticity parameter K. For K values around K_c, characteristic peculiarities such as stochastic sea, island chains, KAM surfaces, etc., can be clearly seen in the figures 2 and 3.

Because of the obvious translation symmetry it is convenient to study the topological properties of the phase plane with boundary conditions on torus, i.e., the variables (p, θ) are replaced with the new variables $(\bar{p}, \bar{\theta})$ by substituting

$$\bar{p} = p \bmod 1, \quad \bar{\theta} = \theta \bmod 1, \tag{8}$$

such that

$$0 \leq \bar{\theta} < 1\,, \quad -0.5 \leq \bar{p} < 0.5\,. \tag{9}$$

Other choices of boundary conditions originate from the specific applications one has in mind. For example, in plasma physics, the model was extensively used in order to understand generic behavior of field lines and orbit dynamics in partially chaotic as well as completely chaotic magnetic systems. Then, for tokamak applications, in the two-dimensional dynamical system, p can be considered as the "radial" coordinate whereas θ denotes the poloidal angle coordinate [measured in radians divided by 2π]. When studying a "radial", i.e., "action" transport, a natural choice of boundary conditions would be

$$0 \leq \bar{\theta} < 1\,, \quad -\infty < \bar{p} < \infty\,, \tag{10}$$

i.e., operation "mod" is applied only to angle variable.

However, other boundary conditions are also in use. Khodas and Fishman [36] and Khodas *et al.* [37], have used boundary condition on the 1 periodic in p and s periodic in θ torus,

$$\bar{p} = p \bmod 1, \quad \bar{\theta} = \theta \bmod s, \quad s \in \mathbb{N}, \tag{11}$$

to study relaxation rates to invariant density for the kicked rotor.

In this work we investigate the cases of infinite phase space for both θ and p in more detail. To be more specific, we apply two types of boundary conditions,

$$\text{case } A: \quad -\infty < \theta < \infty\,, \quad -\infty < p < \infty\,, \tag{12}$$

$$\text{case } B: \quad -\infty < \theta < \infty\,, \quad -0.5 \leq p < 0.5\,; \tag{13}$$

thus in case B we use p modulo 1.

In the following we shall use Eqs. (6) and (7) together with the just-mentioned restrictions A or B.

As already mentioned, section 2 is devoted to studying a stationary *action* distribution function $\psi(p;\nu) = \langle \psi(p,\theta;\nu) \rangle_\theta$ in framework of the CTRW model.

Due to the translation invariance of the standard map $p'(p,\theta) = p'(p,\theta+N),\ N \in \mathbb{Z}$ it does not matter, what type of angular boundary conditions is used. Therefore in numerical simulations we have enclosed the angle variable on torus θ mod 1. Using the distribution function, an asymptotic mean square displacement may be obtained. The latter is defined in the section 2.3.

The object of our interest in the section 3 will be the transport in the *angular* direction for both cases A and B, i.e., to find, if they exist, corresponding expressions for D_θ and for transport exponent μ_θ. The present investigation deals with the asymptotic behaviors of the system as $K \to \infty$ and $K \to 0$, respectively. Divergences, arising from accelerator mode stable points and other types of stable periodical points will also be discussed.

Let us briefly mention some expected differences between transport in p and θ directions, respectively. First a summary of the p transport. For $K < K_c$, transport barriers in p direction exist in the form of KAM surfaces. Just above the threshold K_c, the system exhibits a very complicated phase space topology. The multiisland structure of the phase plane causes "orbit sticking", which leads to changes in transport rate. The cross section of a capture to the sticky part of the phase space has a very sensitive dependence on K.

By investigations similar to those of White *et al.* [17] one can show a strange (subdiffusive) behavior with strongly varying exponents near threshold. For $K \gg K_c$, as the structures of islands vanish, the transport in p becomes diffusive. The leading order of expression (5) immediately follows from

$$\langle(\Delta p)^2\rangle \sim \frac{(K/2\pi)^2}{4} 2\nu \sim \frac{1}{2\pi^2} D_p \nu \ , \tag{14}$$

where $\Delta p = p_n - p_0$.

Now the different expectations for the (mostly unknown) situation of transport in θ direction. Even for $K < K_c$ we expect a (strong) superdiffusive transport. This expectation is motivated by the following thought experiment. Let $K = 0$ and initial conditions being distributed on p axis as $n(p)\,\delta(\theta)$. After ν

iterations the latter becomes $n(p)\,\delta(\theta-\nu\,p)$. Thus, the mean square displacement shows the following behavior:

$$\begin{aligned}\langle(\Delta\theta)^2\rangle &= \iint \theta^2\, n(p)\,\delta(\theta-\nu\,p)\,dp\,d\theta \\ &= \iint (\nu\,p)^2 n(p)\,dp \;\sim\; \nu^2\,. \end{aligned} \tag{15}$$

Near the threshold K_c we also expect a strange behavior. Extrapolating from the derived variations of the exponents for case B [17], we expect that for the latter case and $K \gg K_c$ the transport may be diffusive. In case A, on the other hand, the transport may be much faster, e.g., $D_\theta \sim D_p\,\nu^2$ (see below).

To analyze the angular transport, here we apply a procedure based on the Frobenius-Perron operator. In the Sec. 3.1, we briefly outline the method. Section 3.3 is devoted to the behavior in the limit $K \to 0$. The opposite limit $K \to \infty$ is considered in two sections. First, we treat case A in Sec. 3.4. The case B is evaluated in Sec. 3.6.

Conclusion and summary follow the main text.

2 Subcritical dynamics of the standard map

2.1 CTRW model

A very important regime in practical applications lies in a domain of moderately large, subcritical values of the stochasticity parameter. For instance, in the tokamak problem, we must be sure that the magnetic field lines (and, hopefully, the plasma) remain confined in the toroidal chamber. In this regime the particles can only be dispersed in a limited region of space, because of the presence of impermeable KAM barriers. This is the reason why in this case the process is *subdiffusive*.

Balescu and co-workers [11, 16] have shown that the motion of the particles in the bounded stochastic region near the separatrix can be approximately described by a *continuous time random walk* (CTRW) [39, 40, 41].

An analysis of a long time series $p(t)$ of a typical chaotic orbit, as in the Fig. 6, suggests that it can be splitted into "basins" of rather regular motion. The three of them are designated in the Fig. 6 with the letters A, B and C. The origin of the basins is strongly related to the well-known *stickiness* phenomenon of the partially chaotic dynamics [42, 43, 44] (see also [15, 17]). Long range correlation effects occur from visits of orbits to boundary layers in the vicinity of island chains and cantori. This property was named a stickiness of islands.

Further we observe a number of (statistically) simple features of the standard map dynamics. The latter can be described as a conditionally regular motion of the particle within a "basin", followed by a jump to another basin, where the motion is again rather regular, etc. Based on this picture, we simplify the present problem of deterministic chaos by considering that its only random features are the transition probabilities between basins and the duration of the sojourn in a given basin. These are precisely the ingredients necessary for the definition of CTRW.

We consider the evolution in time of the coordinate p_t. Any given particle remains in a basin for some time, then jumps abruptly to another basin, etc. We shall not be interested in the details of the motion within a given basin. Rather we assume that the process, starting at a given initial value, is described *statistically*: the motion is then completely defined by the specification of three features:

1. *the location of the relevant basins in the phase space*,
2. *the probability of a sojourn of length t in a given basin*, and
3. *the transition probability between two basins.*

The conception, that the whole "randomness" associated with the deterministic chaos of the standard map is concentrated in the statistics of the jumps between basins, is, of course, a serious simplification of the exact motion. Nevertheless, as the further analysis shows, this approach gives rather good estimate of the averaged statistical values, such as distribution function or mean square displacement.

The first point mentioned above, i.e., the location of the relevant basins, depends on the value of the stochasticity parameter and on the initial condition. We develop here a general analytical formalism which is illustrated by a very simple particular case. In this example, the stochasticity parameter is chosen to be well below the critical threshold, but not too small (in order to produce sufficiently large chaotic regions); specifically, we choose $K = 0.7$. The portion of phase space under consideration is taken as the region bounded by the main island around (0,0) and the nearest undestroyed KAM barriers above ($p > 0$) and below ($p < 0$) this island; a typical chaotic orbit is shown in Fig. 5.

Neglecting the effect of satellite island chains (which are clearly distinguishable in the plot of stochastic sea), we can say that the three surfaces mentioned above, i.e., the edge of the main island and the two nearest KAM barriers, are the most relevant surfaces bounding the chaotic orbit. As a consequence, we

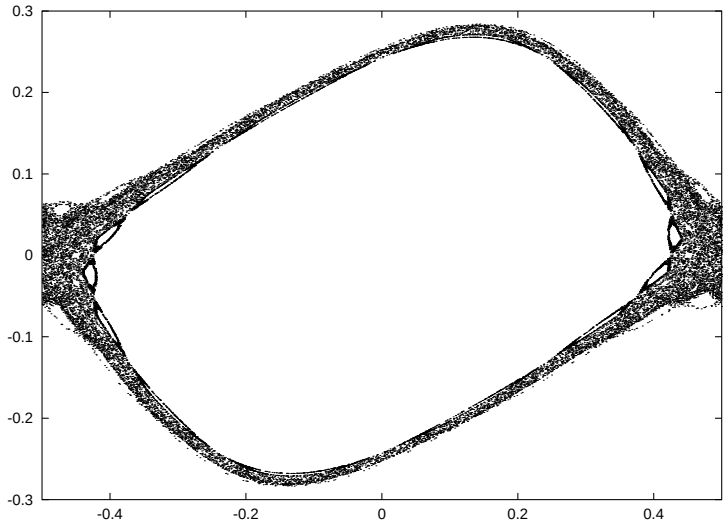

Figure 5: Chaotic orbit for $K = 0.7$ originating from the destroyed separatrix of the main steady island, represented in phase space (p, θ).

expect to observe three basins each corresponding to the motion trapped in the boundary layer of these surfaces.

We now consider a time series, as in Fig. 6. It clearly appears that the p coordinate sojourns successively in three regions: these are the *relevant basins* for $K = 0.7$ and for the present configuration (Fig. 5) of the phase space.

Having identified the relevant basins, we construct a CTRW model describing approximately this dynamics. (A similar, but not identical problem is treated in the monograph [18] under the name "multistate CTRW".) We recall that we are only considering here the distribution of particles among the relevant basins. The latter will be labeled by a subscript, e.g., $m = 1, 2, \ldots, M$, where M is the number of relevant basins in the problem. In our example $M = 3$; the labels are chosen as follows: $m = 1$ for whole island basin; $m = 2$ for that, corresponding to the upper KAM barrier; $m = 3$ - to the lower one.

The random walk (i.e., the "dynamics") is completely determined by the quantities $n_m(t)$: the probability of finding a particle in a basin m at time t. These quantities can be considered as the components of an M-component vector

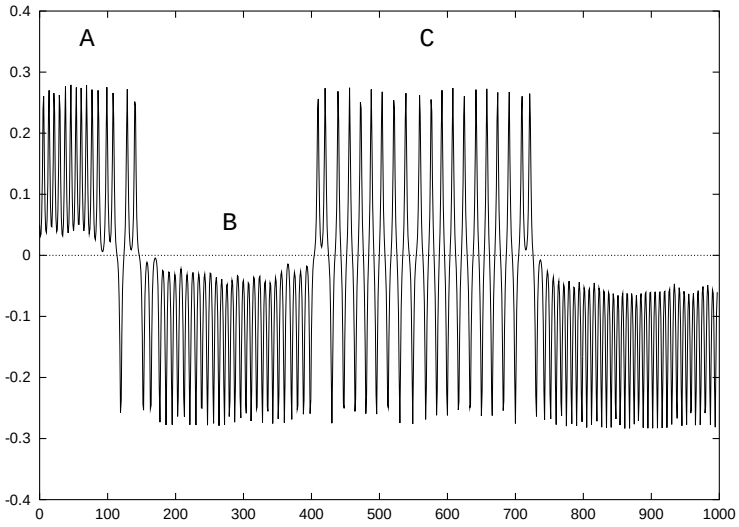

Figure 6: A piece of a chaotic trajectory $p(t)$. Different types of quasi-regular motion, designated as A, B and C, correspond to a sojourn in different basins. C corresponds to motion close to the main island, A and B to upper and lower KAM barriers respectively.

$\mathbf{n}(t)$. We also use the notation $\mathbf{n}^0 = \mathbf{n}(0)$ for the initial condition.

Next, we define $p_m(t)$ as the probability that a particle, entering the basing m, makes a transition after a time t. From the quantities p_m a matrix $P(t)$ can be constructed as follows: $P_{mn}(t) = p_m(t)\delta_{mn}$.

The last component necessary for the definition of the CTRW is the *transition probability* F_{mn} from basin n to basin m: the set of this quantities defines a matrix F. By definition, the diagonal elements are identically zero. Thus, in our example, taking a symmetry reasons into account, we have:

$$F = \begin{pmatrix} 0 & \varphi & \varphi \\ 0.5 & 0 & 1-\varphi \\ 0.5 & 1-\varphi & 0 \end{pmatrix} \tag{16}$$

with $0 < \varphi < 1$. A numerical calculation of the φ leads to the value

$$\varphi \approx 0.616\,. \tag{17}$$

It can be shown (see App. B), that the density $\mathbf{n}(t)$ in Laplace representation yields the following equation:

$$\hat{\mathbf{n}}(s) = \frac{1}{s}\left[I - \hat{P}(s)\right] \cdot \left[I - F \cdot \hat{P}(s)\right]^{-1} \cdot \mathbf{n}^0, \tag{18}$$

where $\hat{P}(s)$ represents a Laplace transform of $P(t)$. This equation provides us with the complete solution of the initial value problem for our CTRW. It is very similar to the well-known *Montroll-Weiss equation* [39, 40, 41] adapted to our problem.

¿From the Eq. (18) a *non-Markovian equation of evolution* for the distribution vector can be obtained:

$$\partial_t \, \mathbf{n}(t) = -(I - F) \cdot \int_0^t d\tau \, Q(\tau) \cdot \mathbf{n}(t - \tau), \tag{19}$$

where the Laplace transform $\hat{Q}(s)$ of $Q(t)$ is given by:

$$\hat{Q}(s) = \int_0^\infty dt \, e^{-st} \, Q(t) = s \, \hat{P}(s) \cdot \left[I - \hat{P}(s)\right]^{-1}. \tag{20}$$

2.2 Asymptotic density distribution

An interesting problem of dynamics of the approach to the saturated steady state is considered in [11, 16]. In this section we will be only interested in the time asymptotic stationary distribution between basins $\mathbf{n}^\infty$. From (19) it is obvious that $\mathbf{n}^\infty$ should satisfy the following equation

$$(I - F) \cdot \left[\int_0^\infty d\tau \, Q(\tau)\right] \cdot \mathbf{n}^\infty = 0. \tag{21}$$

We now present an argumentation, why generally the analytical formula

$$n_m^\infty = \frac{\langle t_m \rangle f_m}{\sum_{\nu=1}^{3} \langle t_\nu \rangle f_\nu} \tag{22}$$

is the correct time asymptotic distribution. Here the f_m denote components of the steady state distribution of the Markov process, that is described by the

transition matrix F (see Eq. (16)). The steady state distribution $\mathbf{f} = (f_1, f_2, f_3)$ is an eigenvector of F corresponding to the eigenvalue 1:

$$(F - I) \cdot \mathbf{f} = 0. \tag{23}$$

It is straightforward to calculate

$$\mathbf{f} \sim \begin{pmatrix} 2\varphi \\ 1 \\ 1 \end{pmatrix}. \tag{24}$$

One heuristic argument for the analytical formula for n_m^∞ is the superposition of two independent processes: waiting in basin m and transition between basins. Let us consider a sequence of transitions. By f_m^T we designate the probability that immediately after the T-th jump the trajectory arrives in basin m. Obviously

$$f_m^{T+1} = \sum_n F_{mn} f_n^T \tag{25}$$

should hold. Thus, in the limit $T \to \infty$ for a stationary distribution, Eq. (23) appears with $f_m^\infty \equiv f_m$.

Next, taking into account the independence of the waiting and transition processes, we conclude that the probability n_m^∞ of finding the system in the state m at arbitrary time should be proportional to the mean waiting time $\langle t_m \rangle$, and therefore

$$n_m^\infty \sim \langle t_m \rangle f_m \,. \tag{26}$$

After a proper normalization, expression (22) is obtained.

Formally, the expression for n_m^∞ can be also found from the asymptotic equation (21). We show first, how the matrix $\mathcal{Q} \equiv \int_0^\infty d\tau\, Q(\tau)$ can be calculated. Performing an inverse Laplace transform, we get:

$$Q(\tau) = \frac{1}{2\pi i} \int_{+\epsilon-i\infty}^{+\epsilon+i\infty} ds\, e^{s\tau}\, \hat{Q}(s)\,, \tag{27}$$

where $\hat{Q}(s)$ is defined in (20). Next integrating $Q(\tau)$ over time, and changing the order of integration, we evaluate:

$$\begin{aligned} 2\pi i \int_0^\infty d\tau\, Q(\tau) &= \lim_{T\to\infty} \int_0^T d\tau \int_{+\epsilon-i\infty}^{+\epsilon+i\infty} ds\, e^{s\tau}\, s\, \hat{P}(s) \cdot \left[I - \hat{P}(s)\right]^{-1} \\ &= \lim_{T\to\infty} \int_{+\epsilon-i\infty}^{+\epsilon+i\infty} ds\, e^{sT}\, \hat{P}(s) \cdot \left[I - \hat{P}(s)\right]^{-1} - \int_{+\epsilon-i\infty}^{+\epsilon+i\infty} ds\, \hat{P}(s) \cdot \left[I - \hat{P}(s)\right]^{-1} \\ &\equiv I_1 - I_2\,. \end{aligned} \tag{28}$$

We calculate these integrals by means of the residue theorem. It can be shown that the only singularity of the $\hat{P}(s)\cdot\left[I-\hat{P}(s)\right]^{-1}$ in the finite part of the s-plane is at $s=0$. For I_1 we can close the contour in the left half of the s-plane, whereas for I_2 we close the contour in the right half of the s-plane. Here we make some assumptions about the asymptotic behavior of the functions $\hat{p}_m(s)(1-\hat{p}_m(s))^{-1}$. They should either have an asymptotic form

$$\frac{\hat{p}_m(s)}{1-\hat{p}_m(s)} \stackrel{s\to\infty}{\longrightarrow} e^{ms}\cdot f(s), \qquad \text{where } m>0 \text{ and } f(s)\to 0, \text{ as } s\to\infty\,,$$

or yield the condition

$$\lim_{s\to\infty} s\,\frac{\hat{p}(s)}{1-\hat{p}(s)} = 0\,.$$

Changing the integration variable $\tilde{s} = -is$, one applies the Jordan's lemma to see that the integral

$$\int_{C_{R_{\text{left}}}} ds\, e^{sT}\, \hat{p}_m(s)\cdot[1-\hat{p}_m(s)]^{-1}$$

vanishes on the left infinite semicircle. Analogously the integral

$$\int_{C_{R_{\text{right}}}} ds\, \hat{p}_m(s)\cdot[1-\hat{p}_m(s)]^{-1}$$

vanishes on the right infinite semicircle.

This leads to

$$I_2 = 0 \quad \text{and} \quad I_1 = -2\pi i\, \text{Res}_{s=0}\left\{ e^{sT}\frac{\hat{P}(s)}{I-\hat{P}(s)}\right\}. \tag{29}$$

To calculate the residue, we expand the Laplace transformation $\hat{P}(s)$ near the origin $s = 0$. Taking into account the normalization condition $\int_0^\infty p(\tau)\, d\tau = 1$ and the existence of the mean waiting times $\langle t_m \rangle = \int_0^\infty \tau\, p_m(\tau)\, d\tau$, we get

$$\begin{aligned} \hat{p}_m(s) &= \int_0^\infty dt\, e^{-st} p_m(t) = \int_0^\infty dt\, (1 - st + \ldots)\, p_m(t) \\ &= 1 - s\langle t_m \rangle + O(s^2)\,, \end{aligned} \tag{30}$$

and, thus, the diagonal elements of the matrix $\hat{P}(s) \cdot \left[I - \hat{P}(s) \right]^{-1}$ become

$$\frac{\hat{p}_m(s)}{1 - \hat{p}_m(s)} \approx \frac{1 - s\langle t_m \rangle + o(s)}{s\langle t_m \rangle + o(s)}\,. \tag{31}$$

The off-diagonal elements are zero. Substituting (31) into (29), we finally get:

$$\mathcal{Q} = \int_0^\infty d\tau\, Q(\tau) = \begin{pmatrix} \langle t_1 \rangle^{-1} & 0 & 0 \\ 0 & \langle t_2 \rangle^{-1} & 0 \\ 0 & 0 & \langle t_3 \rangle^{-1} \end{pmatrix}. \tag{32}$$

But from Eq. (21) we see that vector $\mathcal{Q} \cdot \mathbf{n}^\infty$ yields the equation (23) for the eigenvector of the matrix F, i.e., $\mathcal{Q} \cdot \mathbf{n}^\infty = \mathbf{f}$. From this the Eq. (22) immediately follows.

Explicit expressions for $\mathcal{Q}$ and $\mathbf{n}$ can be found by assuming special functional forms of $p_m(t)$. For instance a piecewise power law

$$p_m(t) = A_m \left[\left(\frac{t}{t_c} \right) \theta(t_c - t) + \left(\frac{t}{t_c} \right)^{-1-\alpha_m} \theta(t - t_c) \right], \tag{33}$$

with $\alpha_m > 1$ and $t_c > 0$. An argumentation for such algebraic decay form may be found in Refs. [45, 16]. Using this form, the average mean waiting times become:

$$\langle t_m \rangle = \frac{2}{3} \frac{\alpha_m}{\alpha_m - 1}\, t_c\,. \tag{34}$$

Now the stationary distribution $\mathbf{n}^\infty$ is defined by the three parameters, φ, α_m and t_c, which can be calculated numerically.

2.3 Mean square displacement

As already mentioned, an adequate way to describe the statistical properties of the chaotic component of the phase space is the *mean square displacement* (MSD): $\langle \Delta p^2(t) \rangle$, where $\langle \cdot \rangle$ means average over initial conditions. Various definitions of the MSD, that are equivalent in diffusive and superdiffusive case, may give different results in subdiffusive regime. Thus we need a correct definition of MSD for every special case.

Let all the initial positions of test particles have the same initial momentum p_0 (but, maybe, different other parameters, such as angle θ_0). The so-defined MSD depends on p_0:

$$\Sigma^2(p_0; t) = \frac{1}{N} \sum_{i=1}^{N} (p_i(t) - p_0)^2. \tag{35}$$

In terms of *distribution function* $\psi(p; t)$ the MSD can be defined as

$$\Sigma^2(p_0; t) = \int (p - p_0)^2 \, \psi(p; t) \, dp. \tag{36}$$

If $p_0 \ll \Sigma^2(p_0; t \to \infty)$ (this is possible in the absence of transport barriers), then the MSD becomes independent of p_0. We will make use of this definition with respect to angle variable in the Sec. 3.

Alternatively, we can put in the phase space pairs of particles with slightly different initial positions in phase space and measure a distance between them:

$$\Sigma^2(t) = \frac{1}{2N} \sum_{i=1}^{N} (p_{1i}(t) - p_{2i}(t))^2, \tag{37}$$

or in terms of distribution function

$$\Sigma^2(t) = \frac{1}{2} \int dp_1 \int dp_2 \, (p_1 - p_2)^2 \, \psi(p_1; t) \psi(p_2; t). \tag{38}$$

An additional factor $1/2$ is chosen so that in the diffusive regime the two definitions above give rise to the same result. In the present chapter we make use of the

second definition (37,38), since it is more suitable for the case of a nonsymmetric distribution (although in our special example the distribution is symmetric, the CTRW model describes the behavior of any weakly chaotic region with not necessarily symmetric distribution).

If a transport barrier exists, the MSD will necessarily saturate to its asymptotic value. An interesting topic is, how the MSD approaches the asymptotic value. It is related to that of relaxation to invariant density distribution, considered by Khodas *et al.* [37]. In this chapter we restrict our consideration only to the saturated state.

We now introduce a way, how the asymptotic probability distribution function $\psi(p;\infty) \equiv \psi(p)$ can be estimated within the framework of CTRW model.

The phase portrait of the trajectories near the discussed region is very similar to that of ordinary mathematical pendulum. To see this, consider a continuous time mechanical system with "kicked rotor" Hamiltonian:

$$H = \frac{p^2}{2} - \frac{K}{4\pi^2}\cos(2\pi\theta)\sum_{\nu}\delta(t-\nu), \tag{39}$$

where $\delta(t)$ is a Dirac function. This system may be thought of as a pendulum, that is subjected to a vertical periodic impulsive force, applied at times $t = 0, 1, 2, \ldots$. It is straightforward to check by direct integrating that the coordinates $p(t)$ and $\theta(t)$, taken at times $\nu - 0$ coincide with a discrete time trajectory iterated by standard map. Thus the standard map becomes a surface of section map for the system (39) (see App. A.2).

Using the Poisson summation formula

$$\sum_{\nu=-\infty}^{\infty}\delta(t-\nu) = \sum_{s=-\infty}^{\infty}\cos(2\pi st), \tag{40}$$

the Hamiltonian (39) can be written in the form

$$\begin{aligned} H &= \frac{p^2}{2} - \frac{K}{4\pi^2}\sum_{s}\cos 2\pi(\theta+st) \\ &= \frac{p^2}{2} - \frac{K}{4\pi^2}\cos 2\pi\theta - \frac{K}{4\pi^2}\sum_{s\neq 0}\cos 2\pi(\theta+st). \end{aligned} \tag{41}$$

In such a form the perturbation of the Hamiltonian (i.e., the part, that disappears as $K \to 0$) may be interpreted as an infinite set of correlated harmonic waves with integer frequencies.

Secular perturbation theory shows[1] that each harmonic wave in a perturbation gives rise to the pendulum-like phase portrait in the vicinity of its resonant torus, until this region of phase space is captured by other structures (e.g. chaotic component). The main resonance, that may be recognized in a phase space portrait (Fig. 2 on the page 11) as an island around the elliptic fixed point $(0, 0)$, is caused by the wave in perturbation with zero frequency ($s = 0$). We have explicitly separated this term in the second equality of (41). Thus the mathematical pendulum with the Hamiltonian

$$H = \frac{p^2}{2} - \frac{K}{4\pi^2} \cos 2\pi\theta \tag{42}$$

has, in the neighborhood of the separatrix, a phase portrait very close to that of the standard map, provided the stochasticity parameter is small enough.

It is easy to see that for a regular trajectory $p(t)$ the distribution function can be written up to normalization constant as

$$\psi(p) \sim \frac{1}{|\dot{p}|}, \tag{43}$$

where $\dot{p}$ should be expressed as a function of p. Indeed, consider a particle, that performs a regular periodic motion with arbitrary initial phase. A probability $dP = \psi(p)\, dp$ to find the particle in the momentum interval dp is proportional to the time dt, that the particle spends in this interval. Thus we have $\psi(p)\, dp \sim dt$, from which Eq. (43) follows.

For the Hamiltonian (42) straightforward calculation leads to

$$|\dot{p}| = \sqrt{\frac{K^2}{4\pi^2} - \pi^2 (p^2 - \frac{K}{2\pi^2} - 2\epsilon)^2}\,, \tag{44}$$

where we have substituted $H = \frac{K}{4\pi^2} + \epsilon$. A small positive ϵ corresponds to a rotation and $\epsilon < 0$ corresponds to a libration.

[1] See Lichtenberg [2], secular perturbation theory.

We now choose three regular orbits of the pendulum by specifying an appropriate ϵ and calculate corresponding distributions ψ_ν. We assume that they estimate distributions in the corresponding basins of the standard map. The total ψ function is constructed in the form

$$\psi(p;t) = \sum_{\nu=1}^{3} n_\nu(t)\psi_\nu(p)\,. \tag{45}$$

This approximation is applicable as long as the mean waiting times $\langle t_\nu \rangle$ are much bigger than the liberation or rotation periods.

Figure 8 shows the analytical distribution ψ, constructed in accordance with (45). When compared to the numerically calculated distribution, Fig. 7, we recognize a quite good agreement. This result could still be improved, if we had considered in our CTRW model more basins. For example those, corresponding to the satellite island chain, which appears nearby the main island and is good recognizable in the phase space portrait in the Fig. 5.

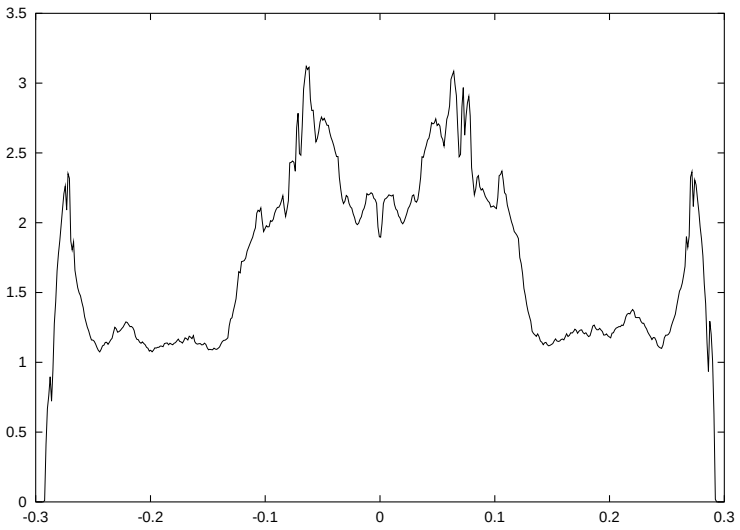

Figure 7: A distribution function $\psi(p)$ for the chaotic region, as in Fig. 5, for $K = 0.7$. The data was obtained from 10^8 iterations of a single orbit.

Finally, we calculate the MSD:

$$\Sigma^2(t \to \infty) = \frac{1}{2}\int dp_1 \int dp_2\, \psi(p_1)\, \psi(p_2)\, (p_1 - p_2)^2 \approx 0.017\,. \tag{46}$$

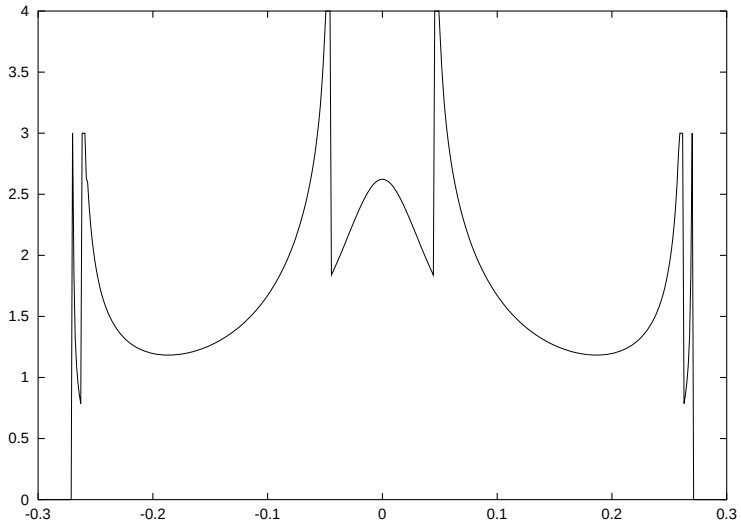

Figure 8: A theoretical estimate of $\psi(p)$. We have truncated peaks, corresponding to integrable singularities of the function $\psi(p)$ appearing on the ages p_{max} and p_{min} of regular trajectories, where $\dot{p} = 0$.

To check the validity of this result we have fulfilled a direct numerical calculation of MSD. The value 0.02 was found. We see that it is in a satisfactory agreement with the value predicted.

3 Angular transport

3.1 Outline of the method

In this section we summarize the definitions and formulas of the Frobenius-Perron operator formalism that are necessary for an understanding of the main results of the present investigation. For reasons of simplicity, we choose here case A (see Eq. (12)), for demonstration.

Suppose we have a discrete time system, whose evolution is governed be a map M. Let also suppose, that there is some distribution of the ensemble of points in the phase space, which is characterized by a distribution function at some initial time $\nu = 0$, $f_0(p, \theta)$. Then, after one time step, the distribution changes because the particles move in accordance with the map M. We denote the distribution function after νth application of the map by $f(p, \theta; \nu)$. The thereby defined (coarse-grained) distribution function should be smooth in the limit of an infinite ensemble. Although in the case of weak chaos, KAM surfaces prevent orbits from reaching arbitrary values of p, it is assumed that $f(p, \theta; \nu)$ is defined in the whole phase plane (θ, p). A one step evolution of the distribution function $f(p, \theta; \nu)$ is then described by Frobenius-Perron equation:

$$f(p, \theta; \nu) = \iint d^2\boldsymbol{x}\, \delta(\boldsymbol{x} - M(\boldsymbol{x}'))\, f(p', \theta'; \nu - 1)\,, \tag{47}$$

where $\boldsymbol{x} = (p, \theta)$. An integral operator $\hat{U}$ with the kernel $\delta(\boldsymbol{x} - M(\boldsymbol{x}'))$ is called Frobenius-Perron (FP) operator [32, 33, 34]. If the map M is invertible, the corresponding FP operator becomes:

$$f(p, \theta; \nu) = \hat{U} f(p, \theta; \nu - 1) = f(M^{-1}(p, \theta); \nu - 1). \tag{48}$$

A complete time evolution of the distribution function is obtained from the νth power of the FP operator:

$$f(p, \theta; \nu) = \hat{U}^{\nu} f_0(p, \theta). \tag{49}$$

Much information about dynamical system parameters, such as escape rates, Lyapunov exponents, diffusion coefficient, may be obtained from the spectral analysis of the FP operator. In particular, as was already mentioned, the poles of the matrix elements of the resolvent,

$$\hat{R}(z) = \frac{1}{z - \hat{U}} = \frac{1}{z} \sum_{n=0}^{\infty} \hat{U}^n z^{-n}, \tag{50}$$

describe the decay (relaxation) of the distribution function to the invariant density. The relaxation rate is, in turn, related to the diffusion coefficient in the action space.

In the current section we will perform direct calculation of the FP operator in Fourier space for the standard map.

Since in this section we are only interested in angular dynamics, the problem may be essentially simplified by averaging over the momentum. We introduce a local density profile $n(\theta;\nu)$ as an average of $f(p,\theta;\nu)$ over the action variable p,

$$n(\theta;\nu) = \int_{-\infty}^{\infty} dp\, f(p,\theta;\nu)\,. \tag{51}$$

All the subsequent calculations will be done in Fourier space. For the Fourier-transform in θ and p we use the definition

$$\tilde{f}(q,m;\nu) = \int_{-\infty}^{\infty} dp \int_{-\infty}^{\infty} d\theta\, \exp[-2\pi i(pq+\theta m)]\, f(p,\theta;\nu)\,, \tag{52}$$

$$f(p,\theta;\nu) = \int_{-\infty}^{\infty} dq \int_{-\infty}^{\infty} dm\, \exp[2\pi i(pq+\theta m)]\, \tilde{f}(q,m;\nu)\,. \tag{53}$$

Here, q and m are continuous variables, since we define p and θ on the whole plane, and we don't assume the distribution $f(p,\theta;\nu)$ to be periodic.

The Fourier transformation of the density is related to the $q=0$ mode of the Fourier transformation of $f(p,\theta;\nu)$,

$$\tilde{n}(m;\nu) = \tilde{f}(q=0,m;\nu)\,. \tag{54}$$

Evidently the normalization condition

$$\tilde{n}(0;\nu) = \int_{-\infty}^{\infty} dp \int_{-\infty}^{\infty} d\theta\; f(p,\theta;\nu) \equiv 1 \tag{55}$$

must hold (for all ν).

In the statistical theory of transport, the diffusion coefficient is related to the time-dependent mean-square-displacement (MSD). The latter we define via

$$\Sigma_\theta^2(\nu) = \int_{-\infty}^{\infty} d\theta\, \theta^2\, n(\theta;\nu)\,. \tag{56}$$

Thus, Σ_θ^2 is just a second moment of the distribution n. As was already mentioned, Σ_θ^2 tends to $\langle(\Delta\theta)^2\rangle$ for $\nu \to \infty$ (see explanation on p. 30).

It is a well-known fact that the moments of a distribution may be easily obtained from its Fourier transform. A simple calculation leads to

$$\Sigma_\theta^2(\nu) = -\frac{1}{4\pi^2}\,\frac{d^2\,\tilde{n}(m;\nu)}{d\,m^2}\bigg|_{m=0}\,. \tag{57}$$

¿From the formula above we can draw an important conclusion, that only an infinitely small region of $\tilde{n}(m;\nu)$ near $m = 0$ determines the MSD [provided $\tilde{n}(m;\nu)$ is an analytic function]. Obviously, this means that for long times only the lowest m modes of the distribution function determine the MSD. We will later make use of this fact, when studying the time dynamics of the distribution. Indeed, as far as the main point of our interest is the MSD, and not the distribution itself, we will restrict the problem of the time evolution of the distribution function only to the lowest Fourier modes, i.e., we will consider the time propagation of $\tilde{n}(m;\nu)$ in the limit $m \to 0$.

It is natural to define the *running* diffusion coefficient $D_\theta = D_\theta(\nu)$ as a time derivative of the displacement $\Sigma_\theta^2(\nu)$, i.e.

$$D_\theta = 2\pi^2\,\frac{\partial\Sigma_\theta^2}{\partial\nu} = -\frac{1}{2}\,\frac{\partial}{\partial\nu}\;\frac{d^2\,\tilde{n}(m;\nu)}{d\,m^2}\bigg|_{m=0}\,. \tag{58}$$

The factor 2π is chosen so that the expression for D_p obtained from this formula for the case $K \to \infty$ coincides with that in literature [Eq. (5)].

3.1.1 Diffusive regime

If the dynamics were diffusive, the density profile would obey a diffusion equation

$$\partial_t\, n(\theta;t) = \frac{D}{4\pi}\,\frac{\partial^2}{\partial\theta^2} n(\theta;t), \tag{59}$$

which in Fourier space takes the form:

$$\partial_t \, \tilde{n}(m;t) = -D \, m^2 \, \tilde{n}(m;t), \tag{60}$$

(because the Fourier transform of ∂_θ^2 is $-4\pi \, m^2$). The solution of this equation is obviously (for $t = \nu$):

$$\tilde{n}(m;\nu) = e^{-D \, m^2 \, \nu} \, \tilde{n}(m;0) \approx \tilde{n}(m;0) - D \, m^2 \, \nu \, \tilde{n}(m;0) \, . \tag{61}$$

An independent on time constant D is a diffusion coefficient, which can be seen from the formula (58).

3.1.2 What we expect

What will we get in the case of nondiffusive dynamics, when the diffusion coefficient is not a constant, rather it has a power dependence on time? Basing on the formula (57) for the MSD, and taking into account the normalization condition (55), we expect for the power expansion of the density profile the following form:

$$\tilde{n}(m;\nu) = \tilde{n}(m;0) + a_1(\nu) m + a_2(\nu) m^2 + a_3(\nu) m^3 + \cdots \, , \tag{62}$$

$$\text{with} \quad a_2(\nu) \sim \nu^{\mu_\theta} \text{ as } \nu \to \infty \, .$$

Indeed, substitution of this expression into the formula (57) leads to the MSD $[\Sigma_\theta^2(\nu) - \Sigma_\theta^2(0)] \sim \nu^{\mu_\theta}$.

3.2 Propagator for "unmoduled" map

We start with the Eqs. (6,7) together with boundary condition A (i.e., with no periodicity) to calculate the propagator $\hat{U}$ for unmoduled map. We start with the definition (48).

An important fact, which plays a key role in determining the FP operator is that the standard map is invertible. The inverse map may be easily obtained by

expressing (p, θ) in terms of (p', θ'):

$$p = p' + \frac{K}{2\pi} \sin 2\pi(\theta' - p') \,, \tag{63}$$

$$\theta = \theta' - p' \,, \tag{64}$$

Combining Eq. (48) with (63) the FP operator may be determined from

$$\hat{U} f(p, \theta) = f\left(M^{-1}(p, \theta)\right) = f\left(p + \frac{K}{2\pi} \sin 2\pi(\theta - p), \theta - p\right). \tag{65}$$

The Frobenius-Perron operator can thus be expressed explicitly as a simple finite displacement operator

$$\hat{U} = \exp\left(-p\frac{\partial}{\partial\theta}\right) \exp\left(\frac{K}{2\pi} \sin 2\pi\theta \frac{\partial}{\partial p}\right). \tag{66}$$

Next we transform to the Fourier space. This space is spanned by the basis:

$$\langle p, \theta |\, q, m\rangle = \exp[2\pi i(pq + \theta m)] \,. \tag{67}$$

In the Fourier representation, the operator $\hat{U}$ has the matrix elements

$$\begin{aligned} \langle q, m|\hat{U}|q', m'\rangle = \quad & \int_{-\infty}^{\infty} dp \int_{-\infty}^{\infty} d\theta \, \exp\left[-2\pi i(pq + \theta m)\right] \\ & \times \hat{U} \, \exp\left[2\pi i(pq' + \theta m')\right]. \end{aligned} \tag{68}$$

Using these matrix elements, the one-step evolution of the distribution function in Fourier space becomes

$$\begin{aligned} & \tilde{f}(q, m; \nu) = \\ & \int_{-\infty}^{\infty} dq' \int_{-\infty}^{\infty} dm' \, \langle q, m|\hat{U}|q', m'\rangle \, \tilde{f}(q', m'; \nu - 1), \end{aligned} \tag{69}$$

or, for the density profile,

$$\begin{aligned} & \tilde{n}(m; \nu) = \\ & \int_{-\infty}^{\infty} dq' \int_{-\infty}^{\infty} dm' \, \langle q = 0, m|\hat{U}|q', m'\rangle \, \tilde{f}(q', m'; \nu - 1) \,. \end{aligned} \tag{70}$$

A complete description of the dynamics is given by an operator $\hat{U}^\nu$. The solution of the initial value problem in Fourier representation follows as

$$\tilde{f}(q,m;\nu) = \int dq' \int dm' \langle q,m|\hat{U}^\nu|q',m'\rangle \, \tilde{f}(q',m';0) \; . \tag{71}$$

In a similar manner as above one can write the Fourier-transformation of the density as

$$\tilde{n}(m;\nu) = \int dq' \int dm' \langle q=0,m|\hat{U}^\nu|q',m'\rangle \, \tilde{f}(q',m';0). \tag{72}$$

For determining the MSD we need only an evolution of the density profile $\tilde{n}(m;\nu)$. Thus our next aim will be to calculate (or, if it is not possible, to estimate) the projection of the νth power of the FP operator $\langle q,m|\hat{U}^\nu|q',m'\rangle$ on the $q=0$ state.

We introduce a projection operator $\hat{P}$ as follows:

$$\hat{P} := |0,m\rangle\langle 0,m| \; . \tag{73}$$

It projects any vector $|\cdot\rangle$ on the $q=0$ state, so that any matrix element $\langle q,m|\hat{P}\hat{U}^\nu|q',m'\rangle$ is zero for $q \neq 0$. We can say that the operator $\langle q,m|\hat{P}\hat{U}^\nu|q',m'\rangle$ is a time propagator for the density profile. One can show that

$$\begin{aligned} \langle q,m|\hat{P}\hat{U}^\nu|q',m'\rangle \; &= \int dq_1 \cdots \int dm_{\nu-1} \\ \times \langle 0,m|\hat{U}|q_1,m_1\rangle \; &\cdots \langle q_{\nu-1},m_{\nu-1}|\hat{U}|q',m'\rangle \; . \end{aligned} \tag{74}$$

¿From here the analog to path-integral may be seen. Indeed, the matrix element $\langle q_i,m_i|\hat{U}|q_j,m_j\rangle$ can be treated as an amplitude of the transition from (q_j,m_j) state to (q_i,m_i) state. The final amplitude is an integral over the all intermediate states, i.e., over the all possible paths in the $(q,m;\nu)$ space. The only specific feature of our case is that the "time" ν is discrete, and, as we will later see, the space (q,m) as well.

Next we proceed to calculation of the propagator in Fourier representation. It is an important fact of the standard map that the matrix elements of the

Frobenius-Perron operator can be calculated analytically. Substituting (66) into (68), we get for the matrix element:

$$\langle q,m|\hat{U}|q',m'\rangle = \int_{-\infty}^{\infty} dp \int_{-\infty}^{\infty} d\theta\, e^{2\pi i[p(q'-q-m')+\theta(m'-m))]}\, e^{iKq'\sin(\theta-p)}\,. \tag{75}$$

Using the well-known identity with Bessel functions J_l (first kind, lth order)

$$\exp(iz\sin\varphi) = \sum_{l=-\infty}^{\infty} e^{il\varphi}\, J_l(z)\,, \tag{76}$$

and performing the integration, one obtains

$$\langle q,m|\hat{U}|q',m'\rangle = \tag{77}$$
$$J_{m-m'}(q'K)\,\delta(q+m-q') \prod_{l=0,\pm1,\ldots} \delta(m-m'-l)\,.$$

Although m and m' are continuous, the difference $m-m'$ remains integer. This reflects the fact, that the Frobenius-Perron operator is invariant under translation transformations $\tilde{\theta} = \theta + n,\ n \in \mathbb{Z}$.

Making use of the explicit form (77), integration over q' and m' can be replaced by summation in following way:

$$\iint dq'\,dm'\,\delta(q+m-q') \prod_{l=0,\pm1,\ldots} \delta(m-m'-l)\,\cdots$$
$$\to \sum_{l} \delta_{q',\,q+m}\,\delta_{m',\,m-l}\,\cdots \tag{78}$$

Thus, we can write for the one-step evolution

$$\tilde{f}(q,m;\nu) = \int dq' \int dm' \langle q,m|\hat{U}|q',m'\rangle \tilde{f}(q',m';\nu-1) = \tag{79}$$
$$\sum_{l=0,\pm1,\ldots} J_l(q'K)\,\tilde{f}(q'=q+m,\ m'=m-l;\ \nu-1)\,.$$

This formula may be interpreted as follows. The state at the moment ν is a sum of transitions from the countable number of the "initial" states (at the moment $\nu-1$) specified by the whole number l, each with the amplitude $J_l(q'K)$. To run

a few steps forward we note that if $q'K \ll 1$, the largest amplitude is given by the choice $l = 0$.

Introducing new indices $k_i = m_i - m,\ i = 1, \ldots, \nu - 1$ and keeping in mind an integration over q' and m' (i.e., we replace the δ-functions with Kronecker delta in accordance with Eq. (78)), the propagator finally becomes

$$\begin{aligned} &\langle q = 0, m|\hat{P}\hat{U}^{\nu}|q', m'\rangle \ = \\ &\sum_{k_1, k_2, \ldots, k_{\nu-1}} J_{k_0 - k_1}(mK)\, J_{k_1 - k_2}\left[(2m + k_1)K\right] \\ &\times \cdots J_{k_{\nu-1} - k_{\nu}}\left[(\nu m + k_1 + k_2 + \cdots + k_{\nu-1})K\right] \\ &\times \delta_{m',\, k_{\nu} - m}\, \delta_{q',\, \nu m + k_1 + k_2 + \ldots + k_{\nu-1}} \ , \end{aligned} \tag{80}$$

where the $k_i, i = 0, \ldots, \nu$, are integers with $k_0 = 0$, $k_{\nu} = m' - m$. The indices k_i specify the intermediate states (q_i, m_i) in the sum (74) by the formulas: $m_i = m + k_i,\ q_i = im + k_0 + k_1 + \cdots + k_{i-1}$.

If we do not specify q' and m', i.e. the matrix element, then each string $k_1, \ldots, k_{\nu}$ determines to which matrix element the corresponding term in the sum (80) contributes. On the other hand, for a given matrix element the two conditions

$$q' = \nu m + k_1 + \cdots + k_{\nu-1}, \tag{81}$$

$$m' = k_{\nu} + m, \tag{82}$$

must hold.

The matrix element $\langle q = 0, m|\hat{P}\hat{U}^{\nu}|q', m'\rangle$ is an amplitude of the transition from the state $(0, m)$ to the state (q', m'). A string of k_i determines a path in the space $(q, m; t)$ as in Fig. 9. The final amplitude is the sum over the contributions from the different paths, each of the magnitude

$$J_{k_0 - k_1}(mK)\, J_{k_1 - k_2}\left[(2m + k_1)K\right] \cdots J_{k_{\nu-1} - k_{\nu}}\left[(\nu m + k_1 + k_2 + \cdots + k_{\nu-1})K\right] \ .$$

Equation (80) is an exact result that provides the starting point for an asymptotic analysis. In the following sections we estimate the propagator in the limits

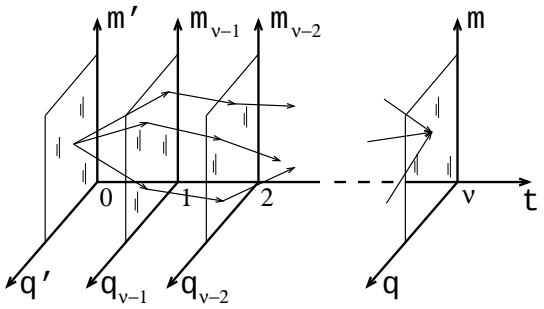

Figure 9: The amplitude of the transition $(0, m) \to (q', m')$ is a sum over different paths in the space $(q, m; t)$.

$K \to 0$ and $K \to \infty$. We show how together with Eq. (72) it leads to the anomalous transport equation (62).

3.3 Asymptotic analysis for $K \to 0$

We shall show now how the transport behavior in θ direction can be obtained from the propagator (80) in the limit $K \to 0$. In Appendix C we present another (simpler) derivation based on the solution of the continuous system of a kicked rotor that corresponds to the discrete standard map.

The propagator (80) consists of a product of Bessel functions. All the arguments $q_i K$ are small in the limit $K \to 0$. We therefore expand the Bessel functions for small arguments in the form

$$J_n(x) = x^n \left[\frac{1}{2^n \, \Gamma(n+1)} - \frac{x^2}{2^{n+2} \, \Gamma(n+2)} + O(x^4) \right] . \tag{83}$$

It is easy to see that the main contribution in the sum (80) originates from the term with

$$k_1 = k_2 = \ldots = k_{\nu-1} = k_\nu = 0 \, . \tag{84}$$

In the case $K = 0$, this is the only nonvanishing term. It is of zeroth order in K; terms with any other choice of k_i contain higher orders of K.

Substituting the string (84) in the expression (80) and using the expansion (83) (in this case all the Bessel functions are $J_0(x) \approx 1$), we get in zeroth order:

$$\langle q, m|\hat{P}\hat{U}^{\nu}|q', m'\rangle = 1 \tag{85}$$

for $q' = \nu m$, and $m' = m$. The solution of the equation of motion (72) becomes

$$\tilde{n}(m;\nu) = \tilde{f}(\nu\, m, m; 0)\,. \tag{86}$$

This is exactly what we get in a corresponding continuous-time system for $K = 0$ (see Appendix C). We conclude that the regime at $K \to 0$ is superdiffusive with respect to angular transport. The corresponding transport exponent $\mu_\theta = 2$. Indeed, using the formulas (57) and (58), the mean square displacement and the diffusion coefficient are:

$$\Sigma_\theta^2 = a \cdot \nu^2\,, \tag{87}$$

$$D_\theta = b \cdot \nu\,, \qquad \nu \to \infty\,, \tag{88}$$

where constants a and b depend on the initial distribution (see Eqs. (211) and (212)). This is obvious from the physical point of view. At $K = 0$ the "orbits" do not change their momenta p at all. So the rate of transport depends only on how the orbits are initially distributed in p. The transport exponent follows from (87) immediately.

We note that, after expanding of the right-hand side of Eq. (86) in power series, the anomalous transport equation (62) with $a_2(\nu) \sim \nu^2$ appears. It should be emphasized that the predicted value $\mu_\theta = 2$ (for $K < K_c$) holds for both cases A and B. In Figs. 10 (p. 49) and 13 (p. 60) it can be easily seen, that the transport exponent remains constant ($\mu_\theta = 2$) up to the stochasticity parameter values $K \leq K_c$, where $K_c \approx 0.97$ is the threshold value. This can be understood from the observation, that the dominant contribution to the transport is made by the particles, located on KAM surfaces.

3.4 Asymptotic analysis in the limit $K \to \infty$ for the case A

Here our aim is to find a diffusion coefficient in the limit $K \to \infty$, when a strong chaos sets in the system. Given the solution $\tilde{n}(m;\nu)$, we have to differentiate it twice at $m = 0$, to obtain the MSD as well as the diffusion coefficient. As was already mentioned, this implies, that the behavior of $\tilde{n}(m;\nu)$ is of interest only in a small region near 0. Thus, the limit $m \to 0$ may be applied, when calculating the propagator. The two limits above are to be applied in the following order. First, we consider large values of K. But after the K is fixed, the limit $m \to 0$ can be applied. In other words, the following two assumptions are crucial. First, we assume a large stochasticity parameter

$$K \gg 1\,. \tag{89}$$

But second, we can assume sufficiently small m, treating K as constant, i.e.

$$mK \ll 1\,. \tag{90}$$

3.4.1 Lowest order in $1/\sqrt{K}$

There are two types of arguments in the Bessel functions of the propagator (80): small ones, if they are like imK, and large ones, if they are like $(im + j)K$, where i, j are integers. Apart from that, we note that for diagonal elements only the terms being proportional to m^2 give a nontrivial contribution to the MSD [see Eq. (57)].

For large arguments we use the expansion

$$J_n(x) = \sqrt{\frac{2}{\pi x}}\left[\cos\left(x - \frac{\pi n}{2} - \frac{\pi}{4}\right) + O(\frac{1}{x})\right]. \tag{91}$$

We shall expand the propagator in a power series of two small parameters, $\sqrt{1/K}$ and mK, respectively. We can immediately proceed with the expressions derived in 3.2. Again, the dominant term in the sum (80) is the one corresponding to the string

$$k_1 = k_2 = \cdots = k_{\nu-1} = k_\nu = 0\,. \tag{92}$$

We shall designate the contribution from this string by S_0. Expanding the Bessel functions up to the second order in mK, we find

$$S_0 = J_0(mK)\, J_0(2mK) \cdots J_0(\nu mK) \approx \left(1 - 1\frac{m^2K^2}{4}\right)\left(1 - 2^2\frac{m^2K^2}{4}\right) \cdots \left(1 - \nu^2\frac{m^2K^2}{4}\right). \tag{93}$$

Up to the second order this product leads to

$$S_0 \approx 1 - \frac{m^2K^2}{4}\sum_{i=1}^{\nu} i^2 = 1 - \left(\frac{\nu}{6} + \frac{\nu^2}{2} + \frac{\nu^3}{3}\right)\frac{m^2K^2}{4}\,. \tag{94}$$

In the next step we consider the transition to large "times" (the limit $\nu \to \infty$ should be taken for fixed K and m),

$$S_0 \approx -\frac{\nu^3}{3}\,\frac{m^2K^2}{4}\,. \tag{95}$$

According to conditions (81) and (82) this contribution belongs to the matrix element of the propagator with $q = 0,\ q' = \nu m,\ m' = m$:

$$\langle 0,\, m|\hat{P}\hat{U}^{\nu}|\nu m,\, m\rangle \approx -\frac{\nu^3}{3}\,\frac{m^2K^2}{4}\,. \tag{96}$$

This is a dominant matrix element of the propagator $\hat{P}\hat{U}^{\nu}$. The equation of motion in first approximation becomes:

$$\tilde{n}(m;\nu) \approx -\frac{\nu^3}{3}\,\frac{m^2K^2}{4}\,\tilde{f}(\nu\, m, m; 0)\,. \tag{97}$$

With the formula (58), this leads to the so called *quasilinear* result:

$$D_{QL} = \frac{K^2}{4}\,, \tag{98}$$

which also may be obtained from a different argumentation (See Introduction).

3.4.2 Next order

The next terms we consider will contain the additional small factor $J_2(K) \sim \sqrt{1/K}$. These terms originate from the strings, which we designate as follows:

$$\begin{aligned} S_i: \quad & k_1 = \cdots = k_{i-1} = 0,\ k_i = 1,\ k_{i+1} = -1, \\ & k_{i+2} = \cdots = k_{\nu-1} = 0; \\ S_{-i}: \quad & k_1 = \cdots = k_{i-1} = 0,\ k_i = -1,\ k_{i+1} = 1, \\ & k_{i+2} = \cdots = k_{\nu-1} = 0; \end{aligned}$$

for $i = 1, 2, \ldots, \nu - 2$. With such a choice of indices the term S_i becomes

$$\begin{aligned} S_i \;=\; & J_0(mK)\, J_0(2mK) \cdots J_0\Big([i-1]mK\Big) \\ & \times J_{-1}(imK)\, J_2\Big([i+1]mK + K\Big)\, J_{-1}\Big([i+2]mK\Big) \\ & \times J_0\Big([i+3]mK\Big) \cdots J_0(\nu mK)\,. \end{aligned} \tag{99}$$

Expanding the Bessel functions, we find that the only principal multiples in the product above are in the middle row. They correspond to that part of the string k_i, where it deviates from the zero. Using the identity $J_{-1}(x) = -J_1(x)$, S_i can be estimated in dominant order as

$$S_i = i(i+2)\,\frac{m^2K^2}{4}\,J_2(K)\,. \tag{100}$$

For S_{-i} we obtain the same expression $S_{-i} = S_i$. Since all these terms contribute to the same matrix element (96), we can add them together, with the result

$$\sum_{i=1}^{\nu-2}(S_i + S_{-i}) = 2\,\frac{\nu^3}{3}\,\frac{m^2K^2}{4}\,J_2(K)\,. \tag{101}$$

Here the summation formula

$$\sum_{i=1}^{\nu-2} i(i+2) = 1 - \frac{5\nu}{6} - \frac{\nu^2}{2} + \frac{\nu^3}{3} \to \frac{\nu^3}{3}\,, \qquad \text{for } \nu \to \infty\,, \tag{102}$$

was used. Combining with S_0, we finally get for this matrix element

$$\langle 0, m|\hat{P}\hat{U}^\nu|\nu m, m\rangle = -\frac{\nu^3}{3}\Big(1 - 2J_2(K)\Big)\,\frac{m^2K^2}{4}\,. \tag{103}$$

We note that for θ transport asymptotically the propagator has off-diagonal elements, and it cannot be represented in the form

$$\langle q, m|\hat{P}\hat{U}^{\nu}|q', m'\rangle \sim \delta(q'-q)\,\delta(m'-m)\,, \tag{104}$$

as it was in the case for "action" diffusion.

The propagator (103) delivers the explicit solution of the equation of motion (72),

$$\tilde{n}(m;\nu) = -\frac{\nu^3}{3}\left(1-2J_2(K)\right)\frac{m^2K^2}{4}\,\tilde{f}(\nu\, m, m; 0)\,. \tag{105}$$

Again we note, that the Eq. (62) with $a_2(\nu) \sim \nu^3$ holds.

Now using Eq. (58), the running diffusion coefficient can be finally estimated as

$$\begin{aligned} D_\theta &\approx \frac{K^2}{4}\left(1-2J_2(K)\right)\nu^2 \\ &\approx \frac{K^2}{4}\left(1+\sqrt{\frac{8}{\pi K}}\cos\left[K-\frac{\pi}{4}\right]\right)\nu^2\,. \end{aligned} \tag{106}$$

We conclude that in case A (Eq. (12)) the angular transport is superdiffusive and the running diffusion coefficient is proportional to ν^2. The corresponding transport exponent in this case $\mu_\theta = 3$. In Fig. 10 one can see that the transport exponent reaches the value 3 for $K \gtrsim 3$.

The "transition" regime, when the stochasticity parameter values are lying in the interval $K_c < K \lesssim 10$, is not described by our approach. In this regime there are no more KAM barriers. This makes the transport in p, and consequently in θ faster, then in subthreshold regime. But the presence of complicated multiisland structure in the phase space causes deviations from the "pure" regimes with integral transport exponent.

Figure 11 shows a comparison of the analytical prediction for the diffusion coefficient with numerical simulations. The oscillations with K can be seen clearly in the plot of $4D_\theta/(\nu^2K^2)$. A quite good agreement is observed for $K \gtrsim 10$.

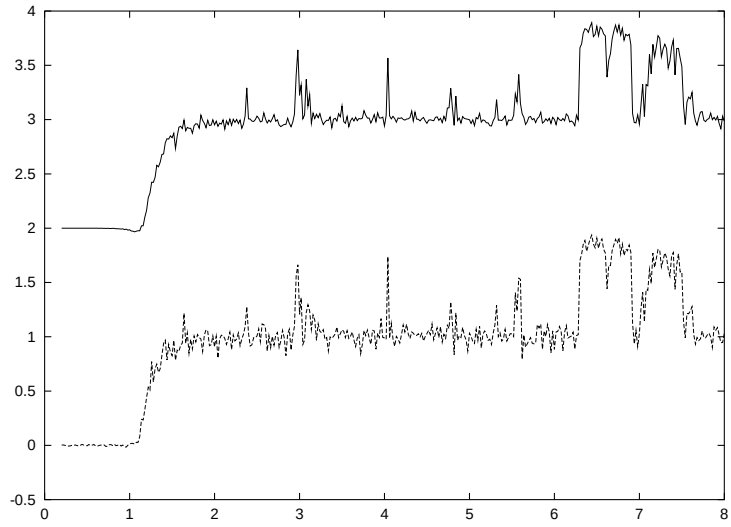

Figure 10: Exponents μ_θ (solid line) and μ_p (dotted line) vs K for case A ($-\infty < p < +\infty$). Note that $\Sigma_\theta \sim \nu^{\mu_\theta}$ and $\Sigma_p \sim \nu^{\mu_p}$. The fluctuation near the value $K \sim 6.5$ is due to influence of accelerator mode islands.

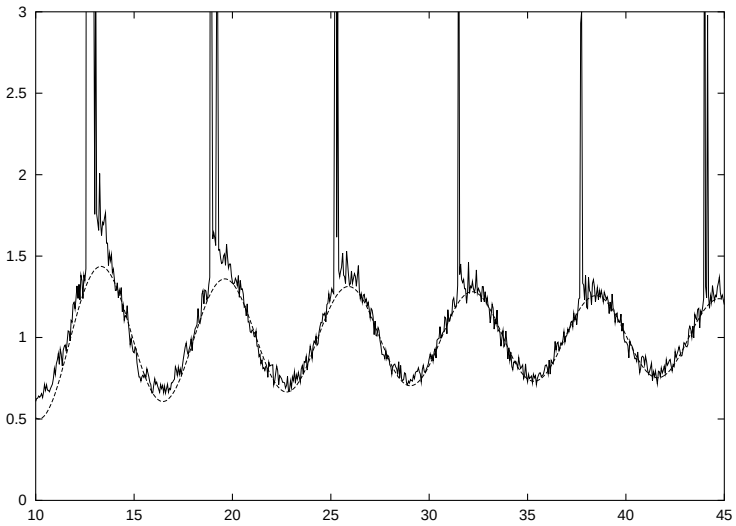

Figure 11: Normalized diffusion coefficient $4D_\theta/(K^2\nu^2)$ vs control parameter K for case A ($-\infty < p < +\infty$). The solid zigzag line represents the measurements from numerical simulations while the dotted curve shows the theoretical prediction.

We note that the angular diffusion coefficient (106) is related to that in action space (5) via

$$D_\theta = D_p \nu^2. \tag{107}$$

In Appendix D we present simple arguments to explain why that should be the case.

3.5 Influence of accelerator mode islands

The present analysis does not apply to the regions around periodical stable points, of which the most important role belongs to the so-called *accelerator modes*. Accelerator mode point is a periodical fixed point of "moduled" map such that, if a trajectory of "unmoduled" map originates in this point, it is displaced in p at every time step by an integer number. Furthermore, if such a point is a stable (elliptical) fixed point of the "moduled" phase space and is surrounded by a KAM island, then the whole island becomes "accelerator mode". In a phase portrait of the "moduled" map the accelerator mode island chains are obviously indistinguishable from ordinary island chains.

Accelerator modes have a very strong influence on the diffusion process. Divergences that may be observed in the $D(K)$ dependence as regular peaks, are related to relatively large "accelerator mode" islands, that appear for certain values of K. Indeed, if a particle appears in an accelerator mode island, it experiences a free acceleration $p \sim \nu$, causing the divergence of the MSD and the diffusion coefficient D.

Let us consider one example. For a period-1 accelerator mode point (p_0, θ_0) [period 1 means that in a "moduled" map it would be a period-1 fixed point] we have the condition

$$-\frac{K}{2\pi} \sin 2\pi\theta_0 \;=\; N\,, \qquad N \in \mathbb{Z}\,; \tag{108}$$

the starting momentum p_0 has to be integer, say 0. The action p, starting in this point, increases at each step by N, and thus grows linearly with time. Then θ

grows as ν^2,

$$p_\nu = p_0 + \nu N = \nu N\,, \tag{109}$$

$$\theta_\nu = \theta_0 + p_1 + \cdots + p_\nu \;\rightarrow\; \frac{\nu^2}{2}\,N\,. \tag{110}$$

Therefore, the mean square displacement in θ direction increases as ν^4. For the transport exponents one gets in these accelerated regions of phase space $\mu_p = 2\,, \quad \mu_\theta = 4$. The relation $\mu_\theta = \mu_p + 2$, discussed in Appendix B, is therefore also valid here. Even when only a few orbits are located in the accelerator mode island, their contribution to the MSD becomes dominant as $\nu \to \infty$.

We should note here that traditionally a strange transport of the chaotic component of the phase space in the vicinity of accelerator mode islands is considered [28, 29, 15]. A fractional anomalous transport exponent was obtained for self-similar configuration of the satellite accelerator mode island chains. Contrary to that consideration our approach deals with a continuous distribution of particles. In particular, some portion of them is located directly on the accelerator mode islands, causing the whole transport exponent to reach the values $\mu_p = 2\,, \quad \mu_\theta = 4$.

A linear stability analysis of the accelerator islands, considered above, shows stability windows

$$\frac{1}{4} - \frac{1}{\pi^2 N} \;<\; \theta_0 \;<\; \frac{1}{4}\,, \tag{111}$$

$$K = \frac{2\pi N}{\sin 2\pi\theta_0}\,. \tag{112}$$

The reason why the accelerator mode contributions were not evident in the propagator expansion is the following: The Fourier modes have been calculated to the lowest order with respect to the small parameter $\sqrt{1/K}$. Contributions of accelerator modes are of higher order in $\sqrt{1/K}$, but contain an additional factor ν. That is why they become dominant as $\nu \to \infty$.

Although the stability windows for the accelerator islands are very narrow, there exist stable accelerator mode islands of higher periods [28]. Their existence

would lead us to the conclusion that divergence should take place for most (probably for all) values of K. In transport simulations that is not observed. As far as we deal with a finite number of orbits, there is a finite probability that an arbitrary orbit can be found in one of the accelerator mode islands. The probability is proportional to the areas occupied by the latter. In turn, these areas (similar to areas of any structures in phase plane) tend to zero as the stochasticity parameter increases. In order to observe the corresponding divergences in computer simulations, either a huge number of orbits with random initial conditions must be taken, or one has to choose some (quite specific) initial conditions on the islands.

To avoid the divergence difficulty, a collision term could be added to the Liouville equation, describing a phase flow of a continuous-time system [30, 37]:

$$\frac{d\,f}{d\,t} = \frac{\partial f}{\partial t} + \{H, f\} = \frac{a^2}{2}\,\frac{\partial^2 f}{\partial \theta^{\,2}}\,, \tag{113}$$

where a^2 characterizes the diffusion process due to collisions. This term leads to an additional factor $\exp(-(a^2/2)\,m^2)$ in the propagator (77). As a consequence, the propagator does not lead anymore to matrix elements with rapid time growth rates caused by accelerator mode (quasi-)periodical orbits. After performing the calculations of the diffusion coefficient, the limit of vanishing noise ($a \to 0$) can be taken to obtain a "physical" solution of the original problem.

3.6 Asymptotic analysis in the limit $K \to \infty$ for case B

We now consider the dynamics of the standard map (6,7) with periodical boundary condition in p, i.e. $-0.5 \le p < 0.5$, $-\infty < \theta < \infty$. Although the phase portrait of this map remains the same as for the "unmoduled" map, the dynamics of particles is quite different. Therefore we need to find a new expression for the propagator of the "moduled" map.

If the operation "mod" is applied to the first equation of the standard map (6), we are immediately faced with a problem that the new map becomes noninvert-

ible. In order to apply the Frobenius-Perron operator formalism, which essentially needs the explicit inversion of the map, let us introduce a function

$$[p] := p \bmod 1\,, \tag{114}$$

where the operation "mod" forces p to the interval $[-0.5, 0.5[$.

Now we can introduce a new map

$$\begin{aligned} p' &= p - \frac{K}{2\pi}\sin 2\pi\theta\,, & (115)\\ \theta' &= \theta + [p']\,, & (116) \end{aligned}$$

which has the same **angular** dynamics as the "moduled" map (Eqs. (6) and (7) with boundary condition $-0.5 \le p < 0.5,\ -\infty < \theta < \infty$). This map may be easily inverted:

$$\begin{aligned} p &= p' + \frac{K}{2\pi}\sin 2\pi(\theta' - p')\,, & (117)\\ \theta &= \theta' - [p']\,, & (118) \end{aligned}$$

Modifying the previous calculations, we get for the Fourier representation of Frobenius-Perron operator

$$\begin{aligned} &\langle q, m|\hat{U}|q', m'\rangle & (119)\\ &= J_{m-m'}(q'K)\int_{-\infty}^{\infty} dp\, \exp(2\pi i\{(q' - q - m + m')p - m'[p]\})\\ &\times \prod_{l=0,\pm1,\ldots} \delta(m - m' - l)\,. \end{aligned}$$

The function $[p]$ can be written as a Fourier series,

$$[p] = \sum_{k=1}^{\infty} \frac{(-1)^{k+1}}{\pi k}\sin 2\pi kp\,. \tag{120}$$

Using this and the summation formula (76), the one-step propagator $\langle q, m|\hat{U}|q', m'\rangle$

becomes

$$\begin{aligned}
&\langle q, m|\hat{U}|q', m'\rangle \qquad (121)\\
&= \sum_{k_1,\, k_2, \ldots} J_{m-m'}(q'K)\, J_{k_1}\left(\frac{2m'}{1}\right)\\
&\times J_{k_2}\left(\frac{2m'}{2}\right) \cdots \prod_{l=0,\pm 1,\ldots} \delta(m - m' - l)\\
&\times \delta(q' - q - m + m' - k_1 + 2k_2 - 3k_3 + \cdots)\ ,
\end{aligned}$$

where the summation indices k_i are integral numbers $k_i \in \mathbb{Z}$.

Next we multiply the propagator ν times to obtain the ν-step propagator

$$\begin{aligned}
&\langle q, m|\hat{P}\hat{U}^{\nu}|q', m'\rangle = \int dq_1 \cdots \int dm_{\nu-1} \qquad (122)\\
&\times \langle 0, m|\hat{U}|q_1, m_1\rangle \cdots \langle q_{\nu-1}, m_{\nu-1}|\hat{U}|q', m'\rangle\ .
\end{aligned}$$

The projection operator $\hat{P}$ was introduced in (73). Again, we have convolutions over all intermediate indices $q_1, m_1, \ldots, q_{\nu-1}, m_{\nu-1}$, which, due to delta functions in (121) may be replaced with summation over integer-valued indices. To be more specific, we introduce an upper sub-index $n = 1, 2, \ldots, \nu$ to specify the transition between the states (q_n, m_n) and (q_{n-1}, m_{n-1}), so that we can substitute:

$$\begin{aligned}
&m_{n-1} - m_n = l^n,\\
&q_n - q_{n-1} = l^n + k_1^n - 2k_2^n + 3k_3^n - \cdots, \quad n = 1, 2, \ldots, \nu
\end{aligned}$$

Using this designation, one finds explicitly

$$\begin{aligned}
&\langle q, m|\hat{P}\hat{U}^{\nu}|q', m'\rangle = \qquad (123)\\
&\sum_{l^1,\, k_1^1,\, k_2^1,\, \ldots} \; \sum_{l^2,\, k_1^2,\, k_2^2,\, \ldots} \cdots \sum_{l^\nu,\, k_1^\nu,\, k_2^\nu,\, \ldots}\\
&\times J_{l^1}(Kq_1)\, J_{k_1^1}\left(\frac{2m_1}{1}\right)\, J_{k_2^1}\left(\frac{2m_1}{2}\right)\, J_{k_3^1}\left(\frac{2m_1}{3}\right)\cdots\\
&\times J_{l^2}(Kq_2)\, J_{k_1^2}\left(\frac{2m_2}{1}\right)\, J_{k_2^2}\left(\frac{2m_2}{2}\right)\, J_{k_3^2}\left(\frac{2m_2}{3}\right)\cdots\\
&\vdots\\
&\times J_{l^\nu}(Kq_\nu)\, J_{k_1^\nu}\left(\frac{2m_\nu}{1}\right)\, J_{k_2^\nu}\left(\frac{2m_\nu}{2}\right)\, J_{k_3^\nu}\left(\frac{2m_\nu}{3}\right)\cdots\\
&\times \delta_{q',\, q_\nu}\, \delta_{m',\, m_\nu}\,, \qquad l^i,\, k_j^i \in \mathbb{Z}
\end{aligned}$$

where we have to substitute

$$\begin{aligned}
q_n &= \sum_{i=1}^{n}(l^i + k_1^i - 2k_2^i + 3k_3^i - \cdots),\\
m_n &= m - \sum_{i=1}^{n} l^i, \qquad n = 1, \ldots, \nu\,.
\end{aligned}$$

Because of the two Kronecker deltas in (123) we have two conditions

$$q' \equiv q_\nu = \sum_{i=1}^{\nu}(l^i + k_1^i - 2k_2^i + 3k_3^i - \cdots), \qquad (124)$$

$$m' \equiv m_\nu = m - \sum_{i=1}^{\nu} l^i\,. \qquad (125)$$

Similar to the case A a choice of the string l^i, k_j^i specifies a path in the (q, m) space, and consequently per Eqs. (124,125) a matrix element where the corresponding term of the sum (123) contributes. On the other hand, for a given matrix element the relations (124,125) must hold. Equation (123) is an exact result. Our next aim will be to find a simplified asymptotic expression for the propagator.

3.6.1 Lowest order in $1/\sqrt{K}$

We consider now the limit $K \to \infty$. Again the two conditions are relevant

$$K \gg 1\,,$$

and

$$mK \ll 1\,.$$

We start with the zeroth order terms (in $\sqrt{1/K}$) in a power series expansion of the propagator. The lowest order follows from the "trivial" choice of all coefficients

$$l^i = k^i_j = 0\,; \qquad i = 1, 2, \ldots, \nu\,;\ j = 1, 2, \ldots\,. \tag{126}$$

Then we get $q_n = 0,\ m_n = m$, for all n. According to Eqs. (124,125) this choice corresponds to the matrix element

$$\langle 0, m|\hat{P}\hat{U}^\nu|0, m\rangle\,, \tag{127}$$

i.e., the dominant matrix element is that with $q' = 0, m' = m$. Substituting (126) in Eq. (123), we get for that matrix element

$$\begin{aligned}
&\langle 0, m|\hat{P}\hat{U}^\nu|0, m\rangle = \\
&J_0\left(\frac{2m}{1}\right)\ J_0\left(\frac{2m}{2}\right)\ J_0\left(\frac{2m}{3}\right)\ \cdots \\
&\times J_0\left(\frac{2m}{1}\right)\ J_0\left(\frac{2m}{2}\right)\ J_0\left(\frac{2m}{3}\right)\ \cdots \\
&\vdots \\
&\times J_0\left(\frac{2m}{1}\right)\ J_0\left(\frac{2m}{2}\right)\ J_0\left(\frac{2m}{3}\right)\ \cdots\,.
\end{aligned} \tag{128}$$

Expanding the Bessel functions for small arguments,

$$J_0(m) \approx 1 - \frac{m^2}{4}\,, \tag{129}$$

we get for each row of expression (128)

$$\begin{aligned}
&J_0\left(\frac{2m}{1}\right)\ J_0\left(\frac{2m}{2}\right)\ J_0\left(\frac{2m}{3}\right)\ \cdots \\
&\approx 1 - m^2 \sum_{i=1}^{\infty} \frac{1}{i^2} = 1 - \frac{\pi^2}{6}\, m^2\ \ .
\end{aligned} \tag{130}$$

In this way, the dominant matrix element (127) becomes, in zeroth order,

$$\begin{aligned} \langle 0, m|\hat{P}\hat{U}^{\nu}|0, m\rangle &\approx \left[1 - \frac{\pi^2}{6}\, m^2\right]^{\nu} \\ &\approx 1 - \frac{\pi^2}{6}\, m^2\, \nu. \end{aligned} \tag{131}$$

Thus, asymptotically the propagator in zeroth order may be written in the form

$$\langle 0, m|\hat{P}\hat{U}^{\nu}|q', m'\rangle \approx \left(1 - \frac{\pi^2}{6}\, m^2\, \nu\right)\, \delta_{q',0}\, \delta_{m',m}\,. \tag{132}$$

Note that the main part of the propagator is diagonal, which is typical for diffusive vortex-free flows. With the propagator (132) the equation of motion has the solution

$$\tilde{n}(m;\nu) = (1 - \frac{\pi^2}{6}\, m^2\, \nu)\, \tilde{n}(m;0)\,. \tag{133}$$

Taking derivative of $\tilde{n}(m;\nu)$ twice with respect to m we get the MSD

$$\Sigma_\theta^2 = -\frac{1}{4\pi^2}\, \frac{\partial^2 \tilde{n}}{\partial m^2}\bigg|_{m=0} = \frac{1}{12}\,\nu\,, \quad \nu \to \infty\,. \tag{134}$$

(We have omitted a constant term, corresponding to the initial distribution $\Sigma_\theta^2(\nu = 0)$).

3.6.2 Next order

Next we consider the first nontrivial choice of coefficients. Let

$$l^i = 0\,;\ k_1^1 = 1\,;\ k_1^2 = -1\,;\ k_1^{i\neq 1,2} = 0\,;\ k_{j>1}^i = 0\,, \quad i - 1, \ldots, \nu\,. \tag{135}$$

This choice contributes to the same matrix element (127). Note that for this choice $q_1 = 1\,;\ q_{i\neq 1} = 0$. In the corresponding contributions to the sum (123) (we designate it by S_1) all but three Bessel functions contribute (in lowest order) with the factor 1. The three principal factors are that containing $k_1^1\,,\ k_1^2$, and q_1. They appear from that part of the string (135), where it deviates from zero. The contribution of this string may be easily estimated:

$$S_1 \approx J_0(K)\, J_1(2m)\, J_{-1}(2m) \approx -J_0(K)\, m^2\,. \tag{136}$$

The further procedure is analogous to that in the previous Sec. 3.4. We can find $2(\nu-1)$ strings with minimal deviation from zero, each contributing to the same matrix element with the same magnitude. We designate these strings, specifying only nonvanishing indices, as follows:

$$\begin{aligned} S_i: &\quad k_1^i = 1,\ k_1^{i+1} = -1\,, \\ S_{-i}: &\quad k_1^i = -1,\ k_1^{i+1} = 1\,, \quad i = 1,\ldots,\nu-1\,. \end{aligned}$$

For all S_i we get the same result as for S_1, i.e., $S_i = S_1 = -J_0(K)\,m^2$, $i = 1,\ldots,\nu-1$. Summing all the terms S_i (remember that all of them belong to the same matrix element (127)), we get

$$\sum_{i=1}^{\nu-1}(S_i + S_{-i}) = 2(\nu-1)S_1 \approx -2\,J_0(K)\,m^2\,\nu\,, \qquad \text{for } \nu \gg 1\,. \tag{137}$$

This is the first order term in the expansion of the propagator. Combining it with the zeroth order term, the propagator finally becomes

$$\langle 0, m|\hat{P}\hat{U}^\nu|q', m'\rangle \approx \left(1 - \frac{\pi^2}{6}\,m^2\,\nu - 2\,J_0(K)\,m^2\,\nu\right)\,\delta_{q',0}\,\delta_{m',m}\,. \tag{138}$$

Now we can write a more precise solution for the equation of motion,

$$\tilde{n}(m;\nu) \approx \left(1 - \frac{\pi^2}{6}\,m^2\,\nu - 2\,J_0(K)\,m^2\,\nu\right)\,\tilde{n}(m;0)\,, \tag{139}$$

from which by virtue of (57) and (58) (as $\nu \to \infty$)

$$\Sigma_\theta^2 = \left(\frac{1}{12} + \frac{1}{\pi^2}\,J_0(K)\right)\,\nu\,, \tag{140}$$

$$D_\theta = 2\pi^2\,\frac{\partial\Sigma_\theta^2}{\partial\nu} = \frac{\pi^2}{6} + 2\,J_0(K) \tag{141}$$

follows. We note again, that, after a proper transformation, the density profile satisfies the predicted analytical asymptotics (62) with $a_2(\nu) \sim \nu$.

Expanding $J_0(K)$ for large arguments, we finally obtain

$$D_\theta = \frac{\pi^2}{6} + \sqrt{\frac{8}{\pi K}}\,\cos\left(K - \frac{\pi}{4}\right)\,. \tag{142}$$

We conclude that the angular transport of the standard map dynamics with periodical boundary conditions (13) is purely diffusive, with transport exponent $\mu_\theta = 1$. The diffusion coefficient is a slightly oscillating function of stochasticity parameter, and asymptotically approaches the constant value $\pi^2/6$.

In Fig. 12 we compare this analytical result with numerical simulations. A very good agreement for $K \gtrsim 10$ is observed.

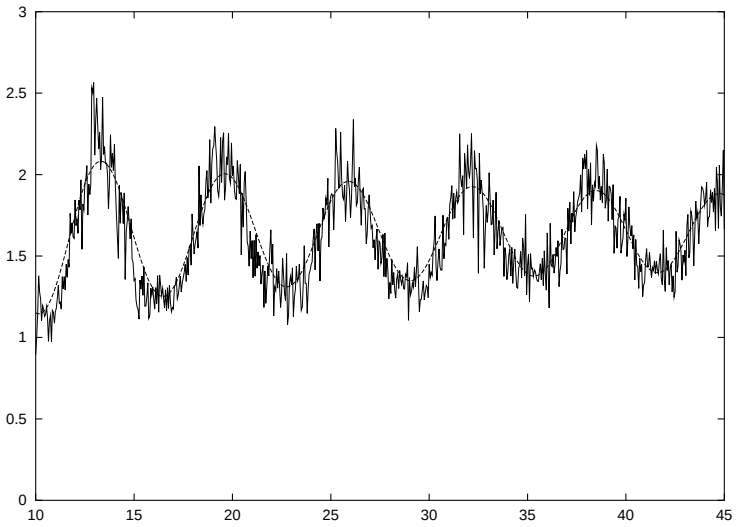

Figure 12: Diffusion coefficient D_θ vs control parameter K for case B ($-0.5 \leq p < +0.5$). The solid line represents the measurements from numerical simulations while the dotted curve shows the theoretical prediction.

In Fig. 13 a numerical calculation of the transport exponents μ_θ and μ_p is shown. One can see that the angular transport exponent reaches the value 1 for $K \gtrsim 3$.

We conclude this section by some heuristic argument, why for the (in p) modulated map diffusion in θ should occur. We base the consideration on the assumption that for large K any p_i can be treated as an arbitrary function of θ_{i-1}. In other words, we assume the existence of a stationary action-density profile $[n_{st}(p) = \langle f(p,\theta)\rangle_\theta,\ (d/dt)n_{st} = 0]$. Within this approximation, p_i is just a random number, distributed in the interval $[-0.5,\ 0.5[$. Let n_{st} has the first

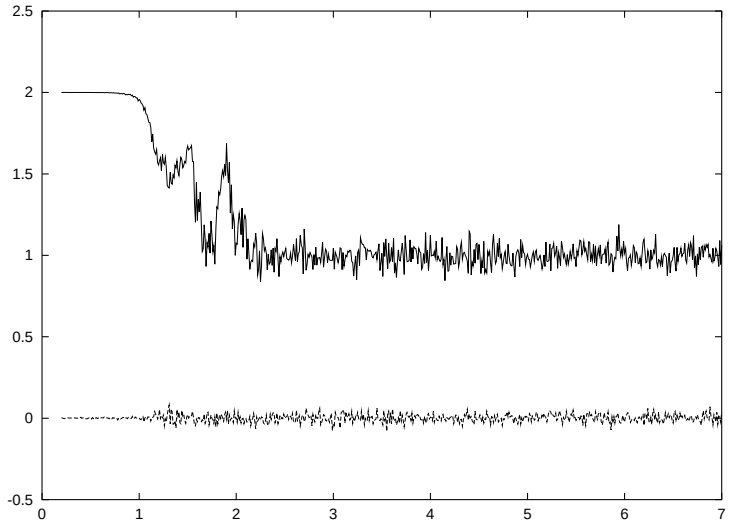

Figure 13: Exponents μ_θ (solid line) and μ_p (dotted line) vs K for case B ($-0.5 \leq p < +0.5$). In the latter case, obviously $\mu_p = 0$.

and second moments $\langle p \rangle = 0$ and σ^2, respectively. Provided p was distributed uniformly, the second moment would be $\sigma^2 = \frac{1}{12}$.

A displacement of a given orbit at time ν is

$$\Delta\,\theta_\nu = \theta_\nu - \theta_0 = \sum_{i=1}^{\nu} p_i \;\approx \theta_\nu . \tag{143}$$

According to the central limit theorem θ_ν should be distributed as

$$P(\theta_\nu) = \frac{1}{\tilde{\sigma}_\nu \sqrt{2\pi}} \exp\left(-\frac{\theta_\nu^2}{2\tilde{\sigma}_\nu^2}\right) , \tag{144}$$

where $\tilde{\sigma}_\nu = \sigma\sqrt{\nu}$. From this distribution function the MSD can be easily obtained as

$$\Sigma_\theta^2 = \int_{-\infty}^{\infty} \theta_\nu^2\, P(\theta_\nu)\, d\theta_\nu = \sigma^2\, \nu\, . \tag{145}$$

For a uniform p distribution (approached in the limit $K \to \infty$) the MSD becomes

$$\Sigma_\theta^2 = \frac{1}{12}\, \nu\, . \tag{146}$$

So, we have a pure diffusive process in agreement with the previous formula. In general, the diffusion rate depends on the p-distribution.

Comparing Eq. (145) with Eq. (140) we conclude that the second moment of the stationary distribution $n_{st}(p)$, i.e. the MSD of action, is an in fact slightly oscillating function of K: $\sigma^2 = \frac{1}{12} + (1/\pi^2)J_0(K)$.

4 Summary and discussion

The first part of the present work was devoted to subcritical dynamics of Chirikov-Taylor (standard) map. It has been shown, that due to the presence of transport barriers an asymptotic stationary coarse-grained **action** distribution function exists.

We used a simplified continuous-time-random-walk model to analyse the stationary action distribution in a chaotic region of the phase space near the primary resonance. The angle variable was assumed to have periodical boundary conditions. In this model it is supposed, that the phase space is divided into several regions, named basins. A given trajectory is reduced to the sequence of sojourns in different basins, followed by transitions to other basins. The only statistical parameters of a trajectory are sojourn-time distribution and transition probabilities.

Making use of the CTRW model, the distribution function was estimated semi-analytically. It has been shown that the asymptotic distribution between basins $\mathbf{n}^\infty$ is proportional to the eigenstate $\mathbf{f}$ of the Markovian process of transitions between basins, and to mean waiting times $\langle t \rangle$. An action distribution function is calculated then as an average over distributions in corresponding basins. In the Figs. 7 and 8 on the page 33 the result of analytical prediction may be compared with computer simulations. Using the distribution function, an asymptotic mean square displacement was explicitly calculated.

In the second part we have investigated the **angular** transport in a nonperiodic standard map. The angular diffusion coefficient was estimated analytically, using Frobenius-Perron operator in Fourier representation.

We have observed superdiffusive behavior for $K \to 0$ with a transport exponent $\mu_\theta = 2$. The transport properties for large values of K ($K \to \infty$) depend on the boundary conditions for the action variable p. For an unrestricted p region (case A, Eq. (12)), the transport is found to be superdiffusive with the transport exponent $\mu_\theta = 3$. The action and angle diffusion coefficients are shown to obey the relation $D_\theta \simeq \nu^2 D_p$. This theoretically predicted behavior is in complete agreement with numerical simulations, as shown in Fig. 11. On the other hand, for a periodic boundary condition in p (case B, Eq. (13)), the θ transport becomes diffusive ($\mu_\theta = 1$), and the corresponding diffusion coefficient has been derived. Again, as shown in Fig. 12, the agreement with numerical simulations is excellent. Thus all analytical predictions are confirmed by numerical simulations. In both cases of periodical and unrestricted boundary conditions, characteristic oscillations in the transport coefficients occur. They appear due to correlations, which persist well above the chaotic threshold. Figures 10 and 13 also contain the results for transport exponents for θ, as well as p diffusion. Figure 10 shows that in case A the accelerator modes have the same influences on both, θ and p transport. In case B (Fig. 13) obviously no divergences due to accelerator modes occur.

A Chaos in Hamiltonian systems

A.1 Definitions of Hamiltonian formalism

In this section we briefly review the most significant principles of the Hamiltonian mechanics, which is an essential part of the dynamical systems theory. As we will see, Hamiltonian mechanics forms a basis for understanding properties of the area-preserving mappings.

Dynamical systems A *dynamical system* may be defined as a deterministic mathematical prescription for evolving the state of a system forward in time. The time-evolution of a N-dimensional dynamical system can be described in terms of N first-order differential equations:

$$\left.\begin{aligned} dx^1/dt &= F_1(x^1, x^2, \ldots, x^N) \\ dx^2/dt &= F_2(x^1, x^2, \ldots, x^N) \\ &\vdots \\ dx^N/dt &= F_N(x^1, x^2, \ldots, x^N) \end{aligned}\right\} \tag{147}$$

or, written in vector form

$$\frac{d\boldsymbol{x}}{dt} = \boldsymbol{F}(\boldsymbol{x}(t))\,, \tag{148}$$

where $\boldsymbol{x}$ is a N-dimensional vector. The space $(x^1, x^2, \ldots, x^N)$ is referred to as a *phase space*. The path in the space followed by the system as it evolves in time is referred to as a *trajectory* or *orbit*. Let us consider an arbitrary point of the phase space M and a solution of the system (147), for which the M is the initial condition at time $t = 0$. The solution at time t depends on M. So we can write

$$M(t) = g^t\, M\,. \tag{149}$$

¿From the ordinary differential equations theory it is known, that, under rather general assumptions about the right-hand-side of the system (147), the mapping $g^t : \mathbb{R}^N \to \mathbb{R}^N$ forms a group of diffeomorphisms: $g^{t+s} = g^t \circ g^s$; g^0 is

an identity element of the group and g^{-t} is inverse to the g^t. This group is called a *phase flow* of the system (147).

Let us consider a "particle", which position in space is specified by N generalized coordinates q^i. A time-dynamics of the system is, as a rule, described by a second order ordinary differential equation. Thus, treating generalized velocities $\dot{q}^i$ as N additional independent coordinates, we obtain a $2N$-dimensional dynamical system of the form (147). This system is said to have N *degrees of freedom*. A phase space of the system is then formed by $2N$ dimensional vectors $\boldsymbol{x} = \{\dot{q}^1, \dot{q}^2, \ldots, \dot{q}^N, q^1, q^2, \ldots, q^N\}$.

Among other dynamical systems the important role belongs to *Hamiltonian* or *symplectic* mechanical systems.

Hamiltonian mechanics A dynamics of a Hamiltonian system [46] is completely specified by a single function, the Hamiltonian $H(\boldsymbol{p}, \boldsymbol{q}, t)$. The state of the system with N degrees of freedom is specified by its "momentum" $\boldsymbol{p}$ and "position" $\boldsymbol{q}$, where $\boldsymbol{p}$ and $\boldsymbol{q}$ are N-dimensional vectors.

The time evolution of the trajectory in $2N$-dimensional phase space is given by Hamiltonian's equations

$$d\boldsymbol{p}/dt = -\partial H(\boldsymbol{p}, \boldsymbol{q}, t)/\partial \boldsymbol{q}\,, \tag{150}$$

$$d\boldsymbol{q}/dt = \partial H(\boldsymbol{p}, \boldsymbol{q}, t)/\partial \boldsymbol{p}\,. \tag{151}$$

Any set of variables $\boldsymbol{p}, \boldsymbol{q}$ whose time evolution is given by the equation of the form (150,151) is said to be *canonical*, with p^i and q^i said to be *conjugate* variables.

By taking $\boldsymbol{x}$ to be $2N$-dimensional vector $\boldsymbol{x} = (\boldsymbol{p}, \boldsymbol{q})$, the Eqs.(150,151) can be written in the form:

$$\dot{\boldsymbol{x}} = I\, dH \equiv I \frac{\partial H}{\partial \boldsymbol{x}}\,, \tag{152}$$

where

$$I = \begin{pmatrix} 0 & -E \\ E & 0 \end{pmatrix} . \tag{153}$$

Then the field $\boldsymbol{H} := I\,dH$ is referred to as *Hamiltonian vector field.* A *Hamiltonian's phase flow* g_H^t is defined as a flow along the Hamiltonian vector field:

$$\left.\frac{d}{dt}\right|_{t=0} g_H^t \boldsymbol{x} = I\,dH(\boldsymbol{x}) . \tag{154}$$

Perhaps the most basic structural property of Hamiltonian's equations is that they are *symplectic*, i.e., the Hamiltonian phase flow g_H^t conserves a symplectic structure on the configurational manifold. This structure is provided by the differentiable 2-form ω^2, which in canonical variables may be written in the form

$$\omega^2 = d\boldsymbol{p} \bigwedge d\boldsymbol{q} = dp_1 \bigwedge dq_1 + \cdots + dp_N \bigwedge dq_N \tag{155}$$

Thus the symplectic property implies

$$(g^t)^* \omega^2 = \omega^2 . \tag{156}$$

Symplectic nature of the Hamiltonian systems endows them with many specific features that differ qualitatively and fundamentally form other systems. We recall some of this features:

1. The *area preservation* property. Generalized to the extended phase space, this becomes a *Poincaré-Cartan theorem.* Let γ_1 and γ_2 are two arbitrary curves, lying on the same tube of trajectories J. Then the theorem states:

$$\oint_{\gamma_1} (\boldsymbol{p}\,d\boldsymbol{q} - H\,dt) = \oint_{\gamma_2} (\boldsymbol{p}\,d\boldsymbol{q} - H\,dt) . \tag{157}$$

   In particular, if γ_1 and γ_2 are both chosen to lie in a surfaces with $q_i = \text{const}$, $i \neq i_k$, $t = \text{const}$, then the preservation of an area in the plane (q_{i_k}, p_{i_k}) under a time map follows:

$$\oint_{\gamma_1} p_{i_k}\,dq_{i_k} = \oint_{\gamma_2} p_{i_k}\,dq_{i_k} . \tag{158}$$

The area preservation property follows from the invariance if the symplectic form ω in the Hamiltonian flow.

2. Hamiltonian's equations also preserve $2N$-dimensional volumes in the phase space. This statement is known as *Liouville's theorem* and follows from the invariance of the form ω^N.

3. The *Poincaré recurrence theorem*, which states that most of trajectories return at some time arbitrarily close to their start point. From the recurrence theorem in particular follows that any regular orbit is either periodical or is everywhere dense on the torus (See below). Another important consequence of this theorem is that Hamiltonian systems does not support attractors.

Integrability By virtue of Eqs. (150,151) a time dependence of any function $F(\boldsymbol{p}, \boldsymbol{q}, t)$ in phase space is given by

$$\frac{dF}{dt} = \frac{\partial F}{\partial t} + \{F, H\}\,, \tag{159}$$

where $\{F, H\}$ denotes a *Poisson bracket*:

$$\{F, H\} = \sum \frac{\partial H}{\partial \boldsymbol{p}} \frac{\partial F}{\partial \boldsymbol{q}} - \frac{\partial H}{\partial \boldsymbol{q}} \frac{\partial F}{\partial \boldsymbol{p}}\,. \tag{160}$$

It is easy to see that $\{F, H\}$ is nothing else but the derivative of F along the vector field $I\,dH$, $\{F, H\} := (\boldsymbol{H} \cdot \nabla)F$.

A function F is said to be a first integral of motion, if it remains constant in the flow, i.e., if its derivative along the Hamiltonian vector field vanishes. By other words, function F is an integral of motion, if and only if the Poisson bracket $\{F, H\}$ vanishes:

$$\{F, H\} = 0\,. \tag{161}$$

Noether's theorem. If a Hamiltonian function survives under a single-parameter group g_F^t corresponding to some function F, then F is a first integral of the system with the Hamiltonian H. Introducing an operator of the derivative along

the field $\mathbf{F}$: $L_{\mathbf{F}} = \mathbf{F}\frac{\partial}{\partial \boldsymbol{x}}$, we note, that equation

$$L_{\mathbf{F}} H = 0 \tag{162}$$

with respect to unknown function F provides a way for searching integrals of motion, but, in general case, does not give an answer on the question, whether they (integrals) exist and how many (if any).

A concept which is essential for the treatment of Hamiltonian flow is that of integrability. A Hamiltonian system with N degrees of freedom is said to be integrable, if there are N independent first integrals in involution (two functions are said to be in involution, if their Poisson bracket vanishes).

$$F_1, \ldots, F_N; \qquad \{F_i, F_j\} \equiv 0 \quad i, j = 1, 2, \ldots, N. \tag{163}$$

Hamiltonian function can be taken as one of the first integrals.

Consider a manifold M_f

$$M_f = \{x : F_i(x) = f_i\,, \quad i = 1, \ldots, N\}. \tag{164}$$

Any orbit with initial conditions on the surface M_f is restricted to "live" (stay) on it, while evolving in time. It can be shown that the manifold M_f is smooth and (if compact) has a topology of a N-dimensional torus T^N

$$T^N = \{(\phi_1, \ldots, \phi_N) \bmod 2\pi\}. \tag{165}$$

The latter is related to the fact that the torus T^N is the only N-dimensional surface, which has smooth non-degenerate tangent field.

This property lies in the basis of *Poincaré surface of section* technique.

Poincaré surface of section. There exists a general technique to reduce a N-dimensional continuous time system to $N-1$-dimensional map called the *Poincaré surface of section*. For illustrative purposes we consider a conservative Hamiltonian system with two degrees of freedom, $N = 2$. Since the system

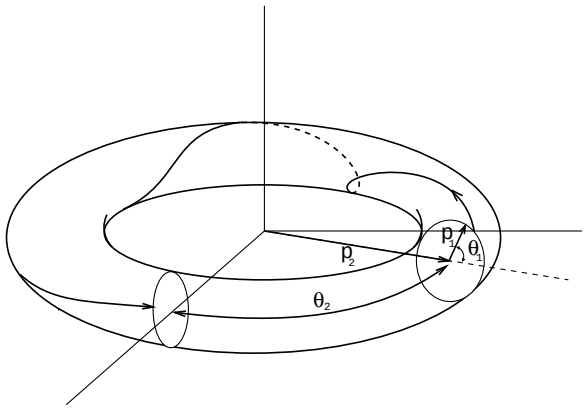

Figure 14: An invariant torus, constructed from the action-angle variables $(p_1, p_2, \theta_1, \theta_2)$. If the frequencies $\omega_i = \partial H/\partial p_i$ are commensurate, the trajectory will be periodic and will repeat itself after some finite time. Otherwise the trajectory will never repeat, but fill the surface of the torus everywhere dense.

is integrable, there exist two isolating integrals of motion, one of which is the Hamiltonian itself:

$$H(p_1, p_2, q_1, q_2) = E, \tag{166}$$

$$I(p_1, p_2, q_1, q_2) = C. \tag{167}$$

The two constants E, C define a two dimensional surface in four dimensional phase space. Any trajectory is restricted to lie on such a surface. Combining Eqs.(166, 167) and choosing q_1 and q_2 as local coordinates on the surface, we can express $p_1 = p_1(q_1, q_2, E, C)$. If we now consider a surface, $q_2 = 0$, the trajectory has to lie on a one dimensional curve. The curve is a cross section of the torus. It is closed (provided the motion is bounded), and two different curves does not cross with one another.

In general if we are given the Hamiltonian (166), we do not know if an additional isolating integral, I, exists. We can check this numerically by solving the

Hamiltonian's equations and plotting p_1 and q_1 each time $q_2 = 0$ and $p_2 \geq 0$. If the system is integrable, the trajectory will appear as a series of points (a mapping) which lie on a one dimensional curve. Otherwise it will occupy some finite (due to energy conservation) area.

A.2 Area preserving maps

Twist maps In case of discrete integer-valued time, an example of a dynamical system is a map, which in vector form is given by

$$\boldsymbol{x}_{n+1} = \boldsymbol{M}(\boldsymbol{x}_n). \tag{168}$$

Say we consider a Hamiltonian system and define the "time T map" $\mathcal{M}_T$ for the system as

$$\mathcal{M}_T(\boldsymbol{x}, t) = \boldsymbol{x}(t + T). \tag{169}$$

This map is symplectic[2], and hence area preserving.

Consider a one-degree-of-freedom system with Hamiltonian, that depends periodically on time: $H(p, q, t) = H(p, q, t + \tau)$, where τ is the period. In that case we can consider our system in an extended phase space by replacing time t with a dependent variable ξ. Since the Hamiltonian is periodic in ξ, we can treat it as an angle variable and replace its value by $\bar{\xi} = \xi$ modulo τ. We then use the surface $\bar{\xi} = t_0$ for our surface of section. Taking in (169) $T = \tau$, we define a surface of section map as a time τ map:

$$\boldsymbol{M}(\boldsymbol{x}) = \mathcal{M}_\tau(\boldsymbol{x}, t_0). \tag{170}$$

It is easy to see that the map $\boldsymbol{M}$ is endowed with the same symplectic properties as $\mathcal{M}_\tau$.

[2] A map $\boldsymbol{M}$ is called symplectic if the matrix $J = \partial \boldsymbol{M}/\partial \boldsymbol{x}$ satisfies the symplectic condition,

$$S = J^\dagger \, S \, J \, ,$$

where † denotes transpose.

A twist map can also be derived from a Poincaré surface of section of the torus. If the system is integrable, the torus is constructed from the action-angle variables $(p_1, p_2, \theta_1, \theta_2)$. The angle θ_2 could play a role of time for time dependent systems. Each time, the trajectory passes a given angle, let us say $\theta_2 = \Theta$, we plot its position in polar coordinates with angle θ_1 and radius $\rho = \sqrt{2p_1}$. The trajectory will thus lie on a circle of radius $\sqrt{2p_1}$. The area enclosed by the circle is $2\pi p_1$. The time interval between passes will be $\tau = 2\pi/\omega_2$ where $\dot{\theta}_2 = \omega_2 = \omega_2(p_1, p_2)$. Let us assume that a given trajectory passes the surface of section at angle $\theta_1 = \phi_n$. Then next time it will pass at angle $\theta_1 = \phi_{n+1} = \phi_n + \omega_1\tau = \phi_n + 2\pi\frac{\omega_1}{\omega_2}$. The quantity $w = \frac{\omega_1}{\omega_2}$ is called the *winding number*. The mapping now takes the form

$$\rho_{n+1} = \rho_n \,, \tag{171}$$

$$\phi_{n+1} = \phi_n + 2\pi w(\rho_n) \,, \tag{172}$$

where w is assumed to be a smooth function of ρ. When a winding number is equal to rational fraction $w = \frac{N}{M}$, where N and M are relatively prime integers, the mapping will consist of M discrete points on a circle. If we denote the initial coordinates of the trajectory as (ρ_0, ϕ_0) then after M iterations of the map we obtain the point$\phi_M = \phi_0 + 2\pi N = \phi_0$ since ϕ is defined mod 2π. Thus the trajectory repeats itself after M iterations, having traveled around the circle N times.

Let us now perturb this map and write

$$\rho_{n+1} = \rho_n + \epsilon f(\rho_n, \phi_n), \tag{173}$$

$$\phi_{n+1} = \phi_n + 2\pi w(\rho_n) + \epsilon g(\rho_n, \phi_n), \tag{174}$$

where f and g are chosen so that area is preserved under the mapping. The area preservation condition is fulfilled if we require that the Jacobian

$$J\begin{pmatrix} \rho_{n+1} & \phi_{n+1} \\ \rho_n & \phi_n \end{pmatrix} = \det\begin{pmatrix} \partial\rho_{n+1}/\partial\rho_n & \partial\rho_{n+1}/\partial\phi_n \\ \partial\phi_{n+1}/\partial\rho_n & \partial\phi_{n+1}/\partial\phi_n \end{pmatrix} = 1 \tag{175}$$

An additional requirement for a twist map is $\partial\phi_{n+1}/\partial\rho_n \neq 0$, so that the twist is always in the same direction.

Standard map The standard map is a single parameter nonlinear twist map which describes the local behavior of nonintegrable dynamical systems in the separatrix region of nonlinear resonances. In the Sec. 2.3 we have shown that it is also a surface of section for a rotor with one degree of freedom, driven by a position dependent, time periodic delta function kick. The standard map may be written in the form:

$$p_{n+1} = p_n - \frac{K}{2\pi}\cos 2\pi\theta_n \mod 1\,, \tag{176}$$

$$\theta_{n+1} = \theta_n + p_{n+1} \mod 1\,, \tag{177}$$

where K is a stochasticity parameter. This map has an obvious translation symmetry $p \to p + n_1, \theta \to \theta + n_2,\ n_1, n_2 \in Z$. For this reason a boundary condition "on torus" (p mod 1, θ mod 1), is usually applied to study the topology of the phase space.

The most of characteristic peculiarities of the twist maps may be demonstrated on example of the standard map. It is often used by many authors to the important features of the transition to chaos in classical conservative systems.

Canonical perturbation theory If a small perturbation is entered in an integrable dynamical system, an approximate solution of the equations of motion may be obtained by means of perturbation theory. Suppose, we can split a Hamiltonian into integrable part and a small perturbation:

$$H = H_0(p_1, p_2) + \epsilon V(p_1, p_2, \theta_1, \theta_2), \tag{178}$$

where ϵ is a perturbation parameter. Variables $(p_1, p_2, \theta_1, \theta_2)$ are the action-angle variables of the unperturbed system. One can try to find new variables $(\bar{p}_1, \bar{p}_2, \bar{\theta}_1, \bar{\theta}_2)$, which were the action-angle variables of the perturbed system.

This would imply, that we have integrated the perturbed system. Let $S(\bar{p}_1, \bar{p}_2, \theta_1, \theta_2)$ be the corresponding generating function. As usually we search for S in the form of perturbation series:

$$S(\bar{p}_1, \bar{p}_2, \theta_1, \theta_2) = \bar{p}_1\theta_1 + \bar{p}_2\theta_2 + \epsilon S_1(\bar{p}_1, \bar{p}_2, \theta_1, \theta_2) + \cdots . \tag{179}$$

Expanding S_1 and V in Fourier series

$$S_1(\bar{p}_1, \bar{p}_2, \theta_1, \theta_2) = \sum_{n_1}\sum_{n_2} S_{n_1,n_2}(\bar{p}_1, \bar{p}_2)\, e^{i(n_1\theta_1 + n_2\theta_2)} \tag{180}$$

$$V(p_1, p_2, \theta_1, \theta_2) = \sum_{n_1}\sum_{n_2} V_{n_1,n_2}(p_1, p_2)\, e^{i(n_1\theta_1 + n_2\theta_2)}\,, \tag{181}$$

we get in the first order:

$$S_{n_1,n_2} = i\,\frac{V_{n_1,n_2}(\bar{p}_1, \bar{p}_2)}{n_1\omega_1 + n_2\omega_2}, \tag{182}$$

where $w_i(\bar{\boldsymbol{p}}) = \partial H_0(\bar{\boldsymbol{p}})/\partial\bar{p}_i$ are the unperturbed angular velocities, taken as functions of $\bar{\boldsymbol{p}} = (\bar{p}_1, \bar{p}_2)$. We are at once faced with a problem of small denominators, since for any $\bar{\boldsymbol{p}}$ an $\boldsymbol{n} = (n_1, n_2)$ can be found such that $n_1\omega_1 + n_2\omega_2$ is arbitrarily close to zero. This may cause the series (180) to diverge, in principle, for any $\bar{\boldsymbol{p}}$, i.e., for any torus, given by $\boldsymbol{\omega} = (\omega_1, \omega_2)$.

We say that an internal resonance occurs, if a condition

$$\boldsymbol{n}\,\boldsymbol{\omega} = n_1\omega_1 + n_2\omega_2 = 0 \tag{183}$$

is fulfilled. Clearly, if the corresponding (resonant) term V_{n_1,n_2} is present in the perturbation, the expansion (180) does not work at all, and the perturbation theory breaks down.

A torus with a winding number $w = \frac{\omega_1}{\omega_2}$ is referred to as a *resonant torus*. We emphasize that the resonant tori are dense in the phase space of the unperturbed Hamiltonian. If resonance occurs in a system , it changes a topology of the phase space trajectories. Qualitatively, these changes are described by the Poincaré-Birkhoff theorem.

For a small perturbation parameter ϵ, resonance layers are thin and separated by nonresonant invariant curves. As ϵ increases, the invariant curves are progressively destroyed, either wrapping up the existing islands or forming chaotic trajectories.

A reason for the chaotic behavior near separatrices may be obtained from the concept of resonance overlap. As the overlap occurs to higher and higher order (islands within islands), the motion becomes exceedingly complicated. This motion is limited to a region near the separatrix by the existence of nearby regular surfaces.

Poincaré-Birkhoff theorem A fate of resonant tori is qualitatively described by Poincaré-Birkhoff theorem. Say, we consider a twist map M. The theorem states, in particular, that perturbation of a torus with winding number $w = \frac{n_1}{n_2}$ results in an equal number of elliptic and hyperbolic fixed points of M^{n_2}.

In the phase portrait of the map the resonant torus appears as an *island chain*, very similar to that of a mathematical pendulum. These islands are also called *resonance zones*. Every island arises around an elliptic fixed point. Such a resonance zone implies a local topological change of the phase space: the separatrix of the resonance splits the space into two parts - inner and outer. For sufficiently small stochasticity parameter, different resonance zones are separated from each other by "survived" regular surfaces, corresponding to nonresonant tori. As the perturbation parameter increases, resonances "absorb" the nearest regular orbits, and thus the area, occupied by resonances increases, too. Resonances may overlap, multiplying the "degree of splitting" of the phase space.

Overlap of an infinite number of resonances leads to appearance of chaotic orbits. The latter are known to fill finite portions of the phase space (provided the stochasticity parameter remains small).

Usually the first candidate to destruction is a separatrix, since an infinite number of resonances usually appears in its vicinity, and a distance between the

successive resonances tends to zero as approaching the separatrix.

Chaotic components of the phase space exhibit a self-similar behavior: a topology of the phase space in the vicinity of secondary resonances is qualitatively similar to that of primary resonances, and this is also valid for all higher order resonances. Thus, not only do we have a dense set of destroyed resonant regions, containing elliptic and hyperbolic orbits, but now we find that these regions of destroyed resonances have embedded within them chaotic orbits. Furthermore, this repeats on all scales as we successively magnify regions around elliptic points.

KAM theory We know that, if a stochasticity parameter is large enough, all the invariant curves, separating the resonance zones are destroyed, and the merging of resonances leads to the appearance of *global* or *strong stochasticity* in the motion. The question, what happens to the system, if the stochasticity parameter remains small, was rigorously studied by Kolmogorov, Arnol'd and Moser.

As we have seen, the canonical perturbation theory diverges (in regions containing resonance zones), if small denominators arise from the resonances. However, Kolmogorov found a way to construct a perturbation theory which was rapidly convergent and applicable to nonresonant tori. Kolmogorov's ideas were made rigorous by Arnol'd and Moser. The nonresonant tori, which have not been destroyed by resonances, are called KAM tori or KAM surfaces (after Kolmogorov, Arnol'd and Moser). Examples of KAM tori can be seen in Fig. 2 on the page 11.

The major result of the KAM theorem is that it guarantees the existence of invariant tori for sufficiently small perturbation parameter. Furthermore, according to KAM theorem, for small ϵ, the perturbed system phase space volume (Lebesgue measure) not occupied by surviving tori is small and approaches zero as ϵ approaches zero.

Fig. 2 shows on example of standard map the most of the typical phase tra-

jectories of a Hamiltonian system. Such a peculiarities as KAM surfaces, island chains and chaotic trajectories may be observed. In the Fig. 3 a regime over threshold is shown, when no more survived primary KAM barriers exist.

B Derivation of the equation for distribution in CTRW

Consider a system, which at given time t can be found in one of M different states. Let the state of the system be described by the M-component distribution vector $\mathbf{n}(\mathbf{t})$: $n_i(t)$ is a probability to find the system at time t in the state i. Dynamics of the distribution vector $\mathbf{n}(\mathbf{t})$ can be described completely, if the two following quantities are known:

- waiting time distribution $\mathbf{p}(t)$. We define $p_i(t)$ as the probability that the system, coming to the state i, makes a transition to another state after a time t. Then the integral $\int_0^t p_i(\tau)\, d\tau$ gives the probability that the system leaves the state i during time t. We define a diagonal $M \times M$ matrix $P(t)$ as

$$\langle m|P(t)|n\rangle = p_m(t)\, \delta_{mn}\,, \tag{184}$$

  without summation in the right-hand-side.

- Transition probabilities f_{mn} from the state n to the state m. These quantities define a matrix F:

$$\langle m|F|n\rangle = f_{mn}\,. \tag{185}$$

By definition the diagonal elements of the matrix F are zero.

The probability $r_i(t)$ that the system, after coming to state i, is still after a time t in the same state, is obviously

$$r_m(t) = 1 - \int_0^t p_m(\tau)\, d\tau\,, \tag{186}$$

or, performing a Laplace transformation,

$$\hat{r}_m(s) = \frac{1}{s}\left[1 - \hat{p}_m(s)\right]. \tag{187}$$

We group these quantities into a diagonal matrix:

$$\hat{R}(s) = \hat{r}_m(s)\,\delta_{mn} = \frac{1}{s}\left[I - \hat{P}(s)\right]. \tag{188}$$

Let $q_m(t)$ be the probability that the system makes a transition to the state m at the time t. Then the probability, that the system is in state m at time t is just a product of the probability $q_m(\tau)$ to arrive to the state m at the time τ times the probability $r_m(t-\tau)$ to stay in this state during the time $t-\tau$, integrated over all intermediate times τ:

$$n_m(t) = \int_0^t d\tau\, q_m(\tau)\, r_m(t-\tau)\,. \tag{189}$$

Using the matrix notation, the last equation becomes in Laplace representation:

$$\hat{\mathbf{n}}(s) = \frac{1}{s}\left[I - \hat{P}(s)\right]\cdot\hat{\mathbf{q}}(s)\,. \tag{190}$$

In order to calculate the quantity $q_m(t)$, we consider successively the cases, where the system arrives to the state m at time t in j steps. For the single jump $j=1$ the probability is obviously:

$$q_m^{(1)}(t) = \sum_k f_{mk}\, p_k(t)\, n_k^0\,, \tag{191}$$

where n_k^0 is the distribution at $t=0$. For $j=2$ the the system first jumps to the state l at time τ, then waits till t and jumps to the state m. The probability $q_m^{(2)}(t)$ is obtained by summing over all intermediate states l and times τ:

$$q_m^{(2)}(t) = \sum_l \int_0^t d\tau\, f_{ml}\, p_l(t-\tau)\, q_l^{(1)}(\tau)\,. \tag{192}$$

Analogously we get a recurrence relation for arbitrary j:

$$q_m^{(j)}(t) = \sum_l \int_0^t d\tau\, f_{ml}\, p_l(t-\tau)\, q_l^{(j-1)}(\tau)\,, \tag{193}$$

which must be solved with the condition

$$q_m^{(0)}(t) = n_m^0\,\delta(t)\,. \tag{194}$$

Written in the matrix form, Eq. (193) becomes

$$\mathbf{q}_m^{(j)}(t) = \sum_l \int_0^t d\tau\, F\cdot P(t-\tau)\cdot \mathbf{q}_l^{(j-1)}(\tau)\,. \tag{195}$$

In Laplace representation the last equation becomes just an algebraic equation:

$$\hat{\mathbf{q}}^{(j)}(s) = F\cdot \hat{P}(s)\cdot \hat{\mathbf{q}}^{(j-1)}(s)\,, \tag{196}$$

which may be easily solved, yielding

$$\hat{\mathbf{q}}^{(j)}(s) = \left[F\cdot \hat{P}(s)\right]^j \cdot \mathbf{n}^0\,. \tag{197}$$

Now, summing this result over j, we get a total probability vector $\hat{\mathbf{q}}(s)$ in Laplace representation:

$$\hat{\mathbf{q}}(s) = \left[I - F\cdot \hat{P}(s)\right]^{-1} \cdot \mathbf{n}^0\,. \tag{198}$$

Substituting this result into Eq. (190), we finally obtain:

$$\hat{\mathbf{n}}(s) = \frac{1}{s}\,\left[I - \hat{P}(s)\right]\cdot \left[I - F\cdot \hat{P}(s)\right]^{-1} \cdot \mathbf{n}^0\,. \tag{199}$$

¿From this result an equation of time evolution for $\mathbf{n}(t)$ can be derived. Using the notation:

$$\hat{Q}(s) = s\,\hat{P}(s)\cdot \left[I - \hat{P}(s)\right]^{-1}\,, \tag{200}$$

we can write:

$$s\hat{\mathbf{n}}(s) - \mathbf{n}^0 = -(I-F)\cdot \hat{Q}(s)\cdot \hat{\mathbf{n}}(s)\,. \tag{201}$$

Performing an inverse Laplace transformation, we get an integral equation of evolution for the distribution vector:

$$\partial_t\,\mathbf{n}(t) = -(I-F)\cdot \int_0^t d\tau\, Q(\tau)\cdot \mathbf{n}(t-\tau)\,. \tag{202}$$

It is easy to see that, if a stationary probability distribution $\mathbf{n}^\infty$ exists, it should satisfy the following equation:

$$(I-F)\cdot \left[\int_0^\infty d\tau\, Q(\tau)\right]\cdot \mathbf{n}^\infty = 0. \tag{203}$$

C Superdiffusion for $K = 0$

Let us consider the continuous Hamiltonian system for the "kicked rotator"

$$H(p, \theta; t) = \frac{p^2}{2} - \frac{K}{4\pi^2} \cos 2\pi\theta \sum_{\nu} \delta(t - \nu) \,. \tag{204}$$

The coordinates $p(t)$ and $\theta(t)$ coincide at $t = \nu - 0$ with p_ν and θ_ν used in the main text. Here, ν stands for the iterated times in the standard map.

In the absence of perturbation ($K = 0$) the continuous system is trivial to integrate. The kinetic equation for the distribution function becomes

$$\frac{\partial f}{\partial t} + p \frac{\partial f}{\partial \theta} = 0 \,. \tag{205}$$

In Fourier space, the corresponding equation

$$\frac{\partial \tilde{f}}{\partial t} - m \frac{\partial \tilde{f}}{\partial q} = 0 \tag{206}$$

has the solution

$$\tilde{f}(q, m; t) = \tilde{F}(m, mt + q) \,, \tag{207}$$

where $\tilde{F}$ is an arbitrary function that can be expressed through the initial distribution,

$$\tilde{f}(q, m; 0) := \tilde{f}_0(q, m) = \tilde{F}(m, q) \,. \tag{208}$$

Thus,

$$\tilde{f}(q, m; t) = \tilde{f}_0(q + mt, m) \,, \tag{209}$$

and for the density profile we obtain

$$\tilde{n}(m; t) = \tilde{f}(q = 0, m; t) = \tilde{f}_0(mt, m) \,. \tag{210}$$

Now Eq. (57) can be applied to estimate Σ_θ^2. Leaving only the dominant term in the large-time limit, it becomes

$$\Sigma_\theta^2 \to -\frac{1}{4\pi^2} \left. \frac{\partial^2 \tilde{f}_0(q', m')}{\partial q'^2} \right|_{\substack{q'=0 \\ m'=0}} t^2 = const \;\; t^2 \tag{211}$$

The first derivative of Σ_θ^2 with respect to time gives the running diffusion coefficient (58), i.e.,

$$D_\theta = - \left. \frac{\partial^2 \tilde{f}_0(q', m')}{\partial q'^2} \right|_{\substack{q'=0 \\ m'=0}} t = const \ t \ . \tag{212}$$

The regime is superdiffusive with the diffusion exponent $\mu_\theta = 2$.

D Relation between angle and action diffusion

Let us start with the assumption that the transport in p direction is diffusive. Then we introduce $n(p;\nu)$ as the density profile at "time" ν. We designate $s(p'-p)$ as the transition probability, i.e., the probability that an "orbit" with momentum p after one iteration will have momentum p'. In an ideal diffusive process, $s(p)$ would be a Gaussian. Actually, not the shape but the width of $s(p)$ affects the dynamics. Although it is not exactly the case for the standard map, for the sake of simplicity we use

$$s(p) = \frac{1}{\sqrt{2\pi}\,\sigma} e^{-\frac{p^2}{2\sigma^2}} , \qquad \tilde{s}(q) = e^{-2\pi^2\sigma^2 q^2} . \tag{213}$$

Here σ^2 is an effective one-step mean square displacement of p.

¿From the standard map one can see that $\sigma = \sqrt{\langle (\Delta p)^2 \rangle} = \sqrt{\langle (K^2/4\pi^2)\sin^2(\theta) \rangle} \sim \frac{K}{\pi\sqrt{8}}$. The stickiness property leads to small (periodical) deviations from the linear dependence $\sigma(K) \sim K$. Having a density profile $n(p;\nu)$ at "time" ν, after one iteration it becomes

$$n(p;\nu+1) = \int dp' \ n(p';\nu)\, s(p-p') \, , \tag{214}$$

or in Fourier space

$$\tilde{n}(q;\nu+1) = \tilde{n}(q;\nu)\, \tilde{s}(q) \, . \tag{215}$$

Starting with an initial distribution $n(p;0) = \delta(p)$, we get after ν iterations

$$\tilde{n}(q;\nu) = \Big[\tilde{s}(q)\Big]^\nu = e^{-2\pi^2\nu\sigma^2 q^2} \, . \tag{216}$$

Thus for action diffusion, using Eq. (57), the MSD is

$$\Sigma_p^2 = \nu\sigma^2\,, \tag{217}$$

as was expected for diffusive regime. From here the action diffusion coefficient

$$D_p = 2\pi^2\sigma^2 \tag{218}$$

follows.

We now interpret this formula in the following way. Knowing the diffusion coefficient D_p, one can estimate the effective p displacement σ. The relation between the transports in p and in θ will be estimated from the second equation of the standard map,

$$\Delta\theta = \theta' - \theta = p'\,. \tag{219}$$

When an "orbit" starts with $\theta_0 = 0$, then $n(\theta_1; 1) = s(\theta_1)$ is nothing else but the probability for this "orbit" to have the coordinate θ_1 at time $\nu = 1$. If during ν steps the "orbit" had successive momenta $p_1, p_2, \ldots, p_\nu$, then its actual coordinate is $\theta_\nu = p_1 + p_2 + \cdots + p_\nu$. The amplitude of this process is $s(p_1)\, s(p_2 - p_1) \cdots s(p_\nu - p_{\nu-1})$. Integrating over all intermediate states, we get the probability for the orbit to have the coordinate θ after ν iterations,

$$\begin{aligned} P_\nu(\theta) = \quad & \int\cdots\int dp_1 \cdots dp_{\nu-1}\; s(p_1) \\ & \times s(p_2 - p_1) \cdots s(p_\nu - p_{\nu-1})\,, \end{aligned} \tag{220}$$

where

$$p_1 + p_2 + \cdots + p_\nu = \theta \tag{221}$$

must hold.

After Fourier transform

$$\tilde{P}_\nu(q) = \tilde{s}(q)\, \tilde{s}(2q) \cdots \tilde{s}(\nu q)\,. \tag{222}$$

Substituting $\tilde{s}(q)$ from Eq. (213) and using the summation formula

$$\sum_{i=1}^{\nu} i^2 = \frac{\nu^3}{3} + \frac{\nu^2}{2} + \frac{\nu}{6} \to \frac{\nu^3}{3}\,, \qquad \text{as } \nu \to \infty\,, \tag{223}$$

we finally get

$$\begin{aligned} \tilde{P}_\nu(q) &= \exp\left(-2\pi^2\,\frac{\nu^3}{3}\,\sigma^2 q^2\right) \\ &= \exp(-2\pi^2\,\sigma_\nu^2\,q^2)\,, \end{aligned} \tag{224}$$

where $\sigma_\nu^2 = (\nu^3/3)\,\sigma^2$. Here $\tilde{P}_\nu(q)$ can be interpreted as a Fourier transform of the angular density profile.

Using Eqs. (57) and (58), the MSD and the diffusion coefficient at "time" ν are

$$\Sigma_\theta^2 = -\frac{1}{4\pi^2}\,\frac{\partial^2}{\partial q^2}\tilde{P}_\nu(q)\bigg|_{q=0} = \frac{\nu^3}{3}\sigma^2\,, \tag{225}$$

$$D_\theta = 2\pi^2\,\nu^2\sigma^2\,, \tag{226}$$

respectively. Comparing Eq. (218) with Eq. (226), we conclude that

$$D_\theta = \nu^2\,D_p\ , \tag{227}$$

from which the relation $\mu_\theta = \mu_p + 2$ for the transport exponents immediately follows. A similar relation was derived by Benkadda *et al.* [15] for the anomalous transport in the vicinity of accelerator mode islands.

References

[1] J. D. Lawson. Some criteria for a power producing thermonuclear reactor. *Proc. of the Physical Society*, **70**:6–10, (1957).

[2] A. J. Lichtenberg and M. A. Lieberman. *Regular and Stochastic Motion.* Springer, New York, (1983).

[3] E. Ott. *Chaos in Dynamical Systems.* Cambridge University Press, Cambridge, (1993).

[4] L. E. Reichl. *The Transition to Chaos.* Springer, New York, (1992).

[5] M. Shlesinger, G. M. Zaslavsky, and J. Klafter. *Nature (London)*, **363**:31, (1993).

[6] B. V. Chirikov. *Phys. Rep.*, **52**:264, (1979).

[7] J. B. Taylor. (unpublished).

[8] A. H. Boozer. *Phys. Fluids*, **27**:2055, (1984).

[9] J. T. Mendonça. *Phys. Fluids, B*, **3**:87, (1991).

[10] J. M. Greene. *J. Math. Phys.*, **20**:1183, (1979).

[11] R. Balescu. *Phys. Rev. E*, **55**:2465, (1997).

[12] R. Balescu. *Statistical Dynamics, Matter out of Equilibrium.* Imperial College Press, Singapore, 1997.

[13] S. S. Abdullaev, K. H. Finken, and K. H. Spatschek. *Phys. Plasmas*, **6**:153, (1999).

[14] S. S. Abdullaev, K. H. Finken, A. Kaleck, and K. H. Spatschek. *Phys. Plasmas*, **5**:196, (1998).

[15] S. Benkadda, S. Kassibrakis, R. B. White, and G. M. Zaslavsky. *Phys. Rev. E*, **55**:4909, (1997).

[16] J. H. Misguich, J.-D. Reuss, Y. Elskens, and R. Balescu. *Chaos*, **8**:248, (1998).

[17] R. B. White, S. Benkaddaand S. Kassibrakis, and G. M. Zaslavsky. *Chaos*, **8**:757, (1998).

[18] L. P. Kadanoff. *Phys. Rev. Lett.*, **47**:1641, (1981).

[19] S. J. Shenker. *Physika D*, **5**:405, (1982).

[20] G. M. Zaslavsky, D. Stevens, and H. Weitzner. *Phys. Rev. E*, **48**:1683, (1993).

[21] G. M. Zaslavsky and S. S. Abdulaev. *Phys. Rev. E*, **51**:3901, (1995).

[22] J. D. Meiss. *Phys. Rev. A*, **34**:2375, (1986).

[23] J. D. Meiss and E. Ott. *Physica D*, **76**:110, (1986).

[24] R. S. MacKay. *Physika D*, **7**:283, (1983).

[25] G. M. Zaslavsky. *Physika D*, **76**:110, (1994).

[26] C. C. F. Karney. *Physika D*, **8**:360, (1983).

[27] Y. H. Inchikawa, T. Kamimura, and T. Hatori. *Physika D*, **29**:247, (1987).

[28] R. Ishizaki, T. Horita, T. Kobayashi, and H. Mori. *Prog. Theor. Phys.*, **85**:1013, (1991).

[29] G. M. Zaslavsky and B. A. Niyazov. *Phys. Rep.*, **283**:73, (1997).

[30] A. B. Rechester and R. B. White. *Phys. Rev. Lett.*, **44**:1586, (1980).

[31] A. B. Rechester, M. N. Rosenbluth, and R. B. White. *Phys. Rev. A*, **23**:2664, (1981).

[32] D. Ruelle. *Statistical Mechanics, thermodynamic Formalism.* Addison-Wesley, Reading, MA, (1978).

[33] D. Ruelle. *Phys. Rev. Lett.*, **56**:405, (1986).

[34] H. H. Hasegawa and W. C. Saphir. *Phys. Rev. A*, **46**:7401, (1992).

[35] H. H. Hasegawa and W. C. Saphir. *Aspects of Nonlinear Dynamics: Solitons and Chaos.* Springer, Berlin, 1991.

[36] M. Khodas and S. Fishman. *Phys. Rev. Lett.*, **84**:2837, (2000).

[37] M. Khodas, S. Fishman, and O. Agam. *Phys. Rev. E*, **62**:4769, (2000).

[38] D. Bénisti and D. F. Escande. *Phys. Rev. Lett.*, **80**:4871, (1998).

[39] E. W. Montroll and G. H. Weiss. *J. Math. Phys.*, **6**:167, (1965).

[40] E. W. Montroll and M. F. Shlesinger. *Studies in Statistical Mechanics*, volume 11. North-Holland, Amsterdam, (1984).

[41] R. Balescu. *Phys. Rev. E*, **51**:4807, (1995).

[42] R. S. MacKay, J. D. Maiss, and I. C. Percival. *Physika D*, **13**:55, (1984).

[43] J. D. Hanson, J. R. Cary, and J. D. Maiss. *J. Stat.Phys.*, **39**:327, (1985).

[44] J. D. Maiss and E. Ott. *Physika D*, **20**:387, (1986).

[45] B. V. Chirikov. *Physika D*, **13**:394, (1983).

[46] V. Arnol'd. *Mathematical methods of classical mechanics.* New York, Springer, (1989).

Acknowledgements

The work was carried out in Institut für Theoretische Phusik I, Heinrich-Heine-Universität Düsseldorf. I express my gratitude to all my colleagues at the institute and friends, who were near me all this time.

I thank Herr Prof. Dr. K. H. Spatschek for providing me with a valuable support during these years, for being always ready to discuss the results, also for careful reading of the manuscript and making proposals on its refinement.

To Herr Zügge I am thankful for the technical support and help in hardware problems, to Herr Wenk for administration of the network and computer serviceability.

I thank Frau Gröters and Frau Gerardi for invaluable help in settling of numerous organizational and bureaucratic problems.

Special thanks go to Sylvie Defrasne, Fabio Mancin, Alexander Posth, Christoph Karle, Tobias Schäfer and Dr. Laedke for the pleasant working atmosphere.

I thank my friends, who have been helping me in numerous subjects. I am especially thankful to Tobias Schäfer and Denis Glushkov for the interesting scientific discussions and for the proofreading of my manuscript.

And of course I gratefully thank my parents and my beloved sister.